available to the Public

Final Report
Contract NAS 2-5473 Mod. 6
Acoustical Properties of a Model Rotor
In Non-Axial Flight
Boeing Document No. D210-10666-2

By

E. Hinterkeuser

Prepared by
Boeing Vertol Company
Philadelphia, Pa.

for

U.S. Army Air Mobility Research
and Development Laboratory
Ames Research Center
Moffett Field, California

and

National Aeronautics and Space Administration

September 15, 1973

TABLE OF CONTENTS

I. INTRODUCTION

The rotational noise of a rotor has been rigorously defined in hover and steady level flight (reference 1) The flight regime of a typical helicopter, however, includes rotor flow regimes in which the flow through the rotor is not steady as in hover, nor at a shallow angle with respect to the rotor disc as in forward level flight. A modification of the noise theory was therefore undertaken in reference 2 which models the rotor rotational noise dependence on flow at various inflow angles to the disc. Expressed another way, the modified theory permits the prediction of rotational noise when the rotor thrust axis is not aligned with the free-stream flow.

The modified rotational noise theory accepts blade loading harmonic decays and lift, drag and radial force magnitudes as measured on an actual rotor at any rotor attitude with respect to the flow streamlines. The purpose of the experiment described in one of the later sections of this report was to derive the blade load harmonic distributions for various axial and non-axial rotor flow conditions and to correlate simultaneously measured acoustic radiation with the theoretical acoustic model.

The following report sections contain a description of the theoretical noise model derivation, of a wind tunnel measurement program of blade pressures and rotor noise, and of the correlation achieved with the proposed modified theory.

degrees, while thrust changed from 126 to 292

pounds.

Data Point 12 exhibits the greatest deviation of the

measured from the predicted noise data. Correlation

is good for data points 6, 7, 8, 11 and 13, the

measured acoustic data being within a 10 dB range of

the predicted scatter. Data Points 9 and 10 exhibit

excellent correlation with theory.

Overall correlation of acoustic data with theory for

this flight condition is very good. There is remark-

ably little scatter in the blade pressure data; but

even so, the higher rotational noise harmonic levels

are very sensitive to slight changes in pressure decay

slope, and exhibit a 10 to 15 dB predicted scatter.

It is interesting to observe in Figures 16 thru 23

that after the on-set of stall (Figure 18), approximately

the tenth through twentieth rotor load harmonics

increase in level relative to the fifth through ninth

harmonic. There is then a sharp drop-off in level near

the twentieth harmonic. This plateau effect in harmonic

level distribution is less pronounced at small rotor

shaft angles (Figures 22 and 23). Minima in harmonic load

load distribution appear to occur near the eighth and

twentieth harmonic. The structure off this harmonic

II. ROTATIONAL NOISE THEORY

The acoustical properties of a rotor are described analytically in this section of the report. The basic mechanism which produces rotational noise is outlined, leading to the development of a simplified far-field mathematical description. This formulation is a review of the rotational noise model developed in reference 2 from which this section is freely borrowed to enhance the reader's comprehension of the objective of the measurement program described in the following section of this report.

ROTOR NOISE GENERATION

The noise generated by an open airscrew VTOL aircraft is typically classified by its generation mechanism. For a VTOL aircraft, driven by turboshaft engines, sound which is generated by aerodynamic forces often dominates in the far acoustic field. This aerodynamic sound includes various types of noise which are commonly classified as rotational noise, vortex noise (also called broad-band noise), and blade slap. Mechanical sources of sound which are produced by the transmission, gearbox, and vibrating components of the aircraft may also

be of importance. Each source of sound has its own distinguishable characteristics. The type of sound which dominates is a function of the relative position between the sound source and the observer, the flight condition of the aircraft and many other factors. Nevertheless, at moderate distances from the rotor-craft, some qualitative judgments about the relative importance of the different sound sources can be made. They are listed below in the order of decreasing importance for far-field considerations:

> Blade slap (if it occurs)
>
> Rotor rotational noise
>
> Rotor vortex noise (broad-band noise)
>
> Gearbox & transmission noise
>
> Turbine engine noise

Blade slap, if it occurs, is definitely the most offensive source of noise. The low frequency characteristic impulsive sound is not attenuated to any great extent by the atmosphere and can be heard at large distances from the source. The main rotor rotational noise is a lower frequency sound which is directly related to the integrated forces acting in the rotor blades. Rotor vortex noise, gearbox noise, and turbine engine noise are of higher frequency and are attenuated much faster by the atmosphere.

6

ANALYTICAL NOISE PREDICTION

The rotational noise produced by a rotor in non-axial flight arises from the action of the rotor forces on the surrounding air. Each element of the rotor has an elemental net force acting on it which may be decomposed into a thrust and a drag force. These elemental forces may be integrated along the rotor blade and around the azimuth to yield the total thrust and torque of the rotor. These elemental blade forces cause an equal, but opposite force to be applied to the medium. Assume, for the moment, that the resulting pressure field on the air in the rotating frame is steady (this assumption is valid for a propeller in axial flight). The pressure measured at any fixed location on the rotor disc appears oscillatory. A sketch of this oscillating pressure field is shown in Figure 1.
The pressure over each blade chord is assumed to be constant in this simplified illustration. The frequency of the oscillating pressure field at a point in the rotor disc plane is proportional to the frequency with which the blades pass that point.
This simplified model of oscillating forces and pressures is the cornerstone of present rotational noise analysis. Gutin (ref. 3) was the first to represent the oscillating force field of a propeller
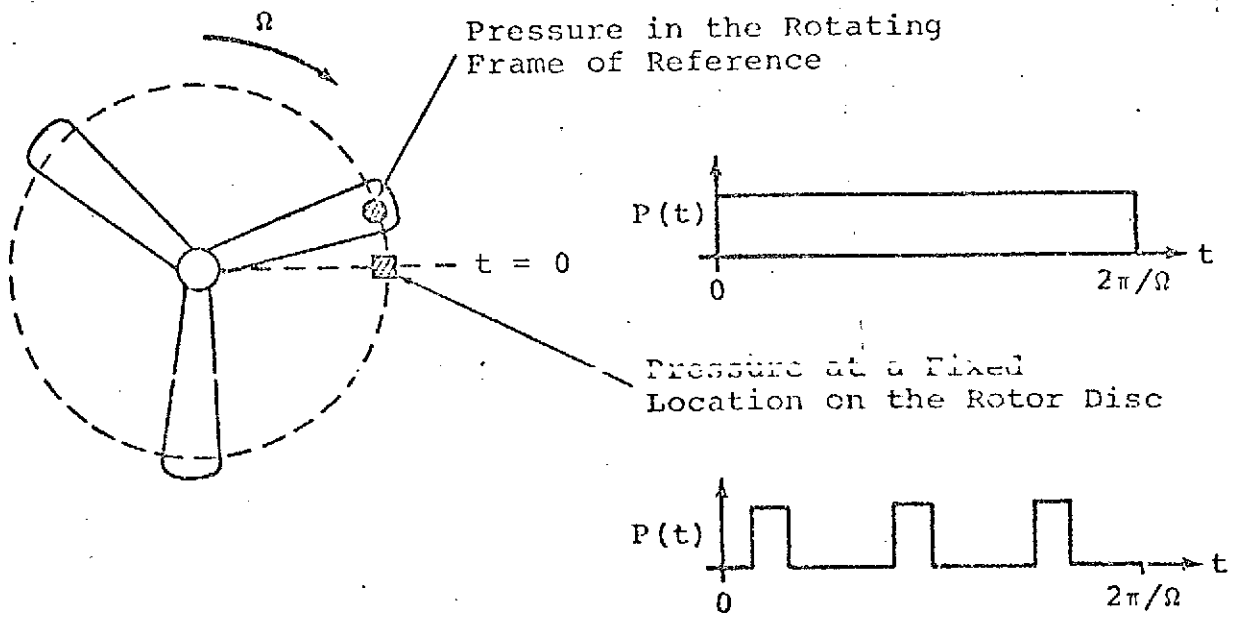
Figure 1.   Oscillating Pressure Field on a Rotor Disc

in a Fourier series. The components of this series
sum to yield the thrust and torque. The rotational
noise of the propeller is determined by treating this
oscillating force field as an array of dipole sources
from which the acoustic field can be calculated.
Garrick and Watkins (ref. 4) extended these concepts
to an axially moving propeller. Because the propeller
is in motion and the observer is stationary, frequency
and retarded time corrections must be applied. In
their derivation, an axis system fixed in the propeller
was assumed.

Recently, Lowson & Ollerhead (refs. 1 and 5) have
presented a theory for helicopter rotational noise
which is very similar to Garrick & Watkin's moving
propeller analysis. They derived their equations in
an axis system fixed in space and included the effect
of rotor coning. Their very complete analysis goes on
to show that helicopter rotational noise is very
dependent upon the higher harmonic airloads. The
pressure field of the air in the rotating frame of a
helicopter is, in general, not steady. The induced
flow field, nonuniform inflow velocities, and nonaxial
translation of the rotor plane all produce time-varying
blade force and pressure fields. They also point out
that an analytic description of the higher harmonic

airloads is presently a formidable, if not impossible, task. However, by curve fitting existing measured and Fourier analyzed airload data (see refs. 6 and 7), Lowson and Ollerhead were able to develop a simplified rotational noise prediction technique that does consider the magnitude of higher harmonic airload data. Their comparison with measured acoustical data was encouraging.

Lowson's basic descriptions (ref.1) have been modified to accommodate arbitrary rotor plane inclinations with respect to an aircraft's velocity and loading laws which are a function of the operating state of the rotor. The theory which results reduced to Garrick and Watkin's analysis when the rotors are acting as conventional propellers in airplane flight. These necessary modifications are presented in the following two subsections of this report.

Acoustic far-field equations: On a rotor craft in non-axial flight, the rotor disc plane may assume any angle with respect to the freestream velocity of the aircraft. A convenient axis system in which to derive the acoustic equations is illustrated in Figure 2 . The chosen set of orthogonal axes are fixed in space at the time the sound was first emitted and the X_n axis is aligned with the thrusting axis of the rotor.
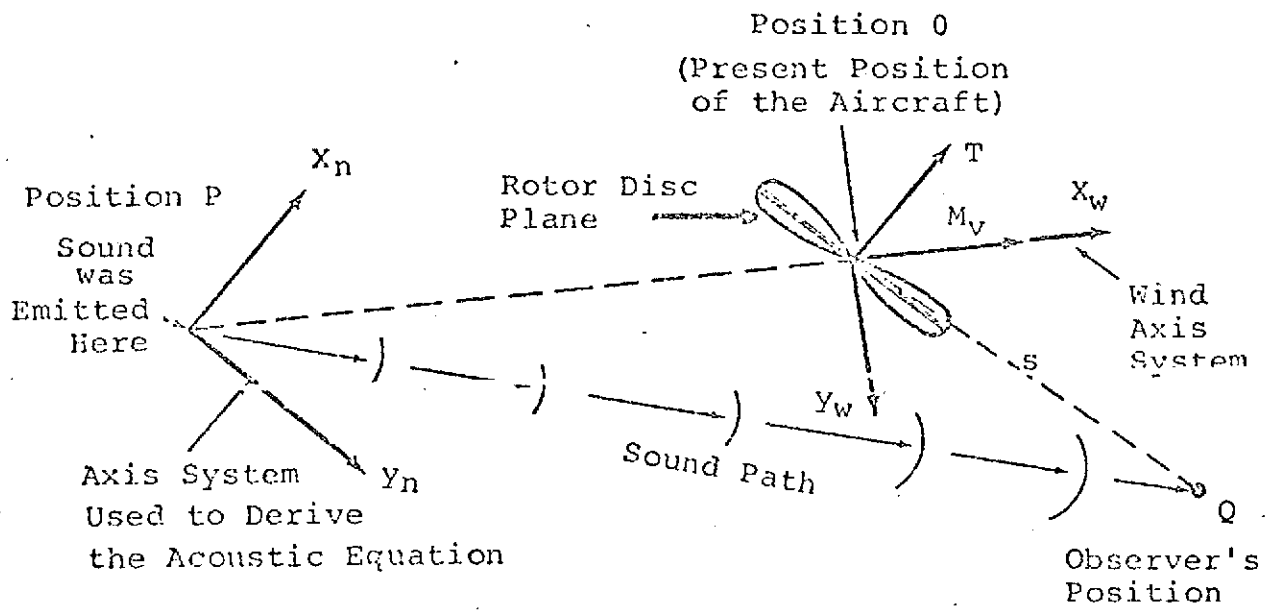
Figure 2.   Orthogonal Axis System used to Derive
the Acoustic Equations

This same axis system was used in the development (ref. 1) of the rotational noise equations of a helicopter operating in level steady-state flight. By differentiating this source in the appropriate directions, the resulting dipole radiation for fluctuating axial, circumferential, and radial components of force can be expressed.

The equation which governs the rotational noise of a rotor operating in non-axial flight becomes, as derived in ref. 1 :

$$C_n = a_n + ib_n$$

$$-\sum_{\lambda=0}^{+\infty} \frac{i^{-(n-\lambda)}}{4\pi}\left\{ \frac{n\Omega X_n}{a_0 s^2}\left| {}_{\pm i a_{\lambda T}}\left(J_{n-\lambda} + (-1)^\lambda J_{n+\lambda}\right) - b_{\lambda T}\left(J_{n-\lambda} - (-1)^\lambda J_{n+\lambda}\right)\right.\right.$$

$$-\left| \frac{ia_{\lambda D}}{R's}\left((n-\lambda)J_{n-\lambda} + (-1)^\lambda(n+\lambda)J_{n+\lambda}\right)\right.$$

$$\left.- \frac{b_{\lambda D}}{R's}\left((n-\lambda)J_{n-\lambda} - (-1)^\lambda(n+\lambda)J_{n+\lambda}\right)\right|$$

$$+ \frac{n\Omega y_n}{a_0 s^2}\left\{ a_{\lambda C}\left(J'_{n-\lambda} + (-1)^\lambda J'_{n+\lambda}\right) + ib_{\lambda C}\left(J'_{n-\lambda} - (-1)^\lambda J'_{n+\lambda}\right)\right\}\right\}$$

$$(II-1)$$

where

C_n = the nth sound harmonic at position Q when the rotor aircraft is presently at 0.

n = mB = harmonic number x number of blades

λ = loading harmonic number

Ω = rotational speed of rotor, radians/sec

X_n = acoustic axis perpendicular to tip path plane with the positive direction forward of the tip path plane

a_c = speed of sound in free air, ft/sec

s = distance of the observer from the rotor hub

$a_{\lambda T}, b_{\lambda T}; a_{\lambda D}, b_{\lambda D}; a_{\lambda C}, b_{\lambda C}$ = the thrust, drag and radial force harmonic components

J = $J(nMy_n/s)$ ≡ Bessel function of argument (nMy_n/s)

R' = radius of point source on rotor

Y_n = acoustic axis parallel to tip path plane with the positive direction below the axis of rotation

J' = derivative of Bessel function

M = Mach number at the radial station of the point source.

13

The root mean square pressure of the nth harmonic

of rotational noise is found by substituting eq.

(II-1) into

$$c_n = (a_n^2 + b_n^2)^{1/2} \qquad (II-2)$$

Lowson & Ollerhead (ref. 1) used eqs. (II-1) and

(II-2) to predict the rotational noise of a heli-

copter operating in level steady-state flight. These

same equations are used in this analysis to predict

the rotational noise of a rotor in non-axial flight.

However, the plane of the rotors is allowed to assume

an angle, αp with respect to the freestream velocity

of the aircraft (see Figure 3).

It is, therefore, necessary to relate the flight

condition of the rotor craft to the X_n, Y_n axis

system. The following geometrical relationships can

be deduced by inspection of Figure 3

$$X_n = X_w \cos (\alpha p) - Y_w \sin (\alpha p) \qquad (II-3)$$

$$Y_n = X_w \sin (\alpha p) + Y_w \cos (\alpha p) \qquad (II-4)$$

$$Z_n = Z_w \qquad (II-5)$$

where
$$X_w = \Delta X_w + Mr \qquad (II-6)$$

$$Y_w = \Delta Y_w \qquad (II-7)$$

and phase radius, $\quad r = \dfrac{M \Delta X_w + S}{\beta^2} \qquad (II-8)$

14
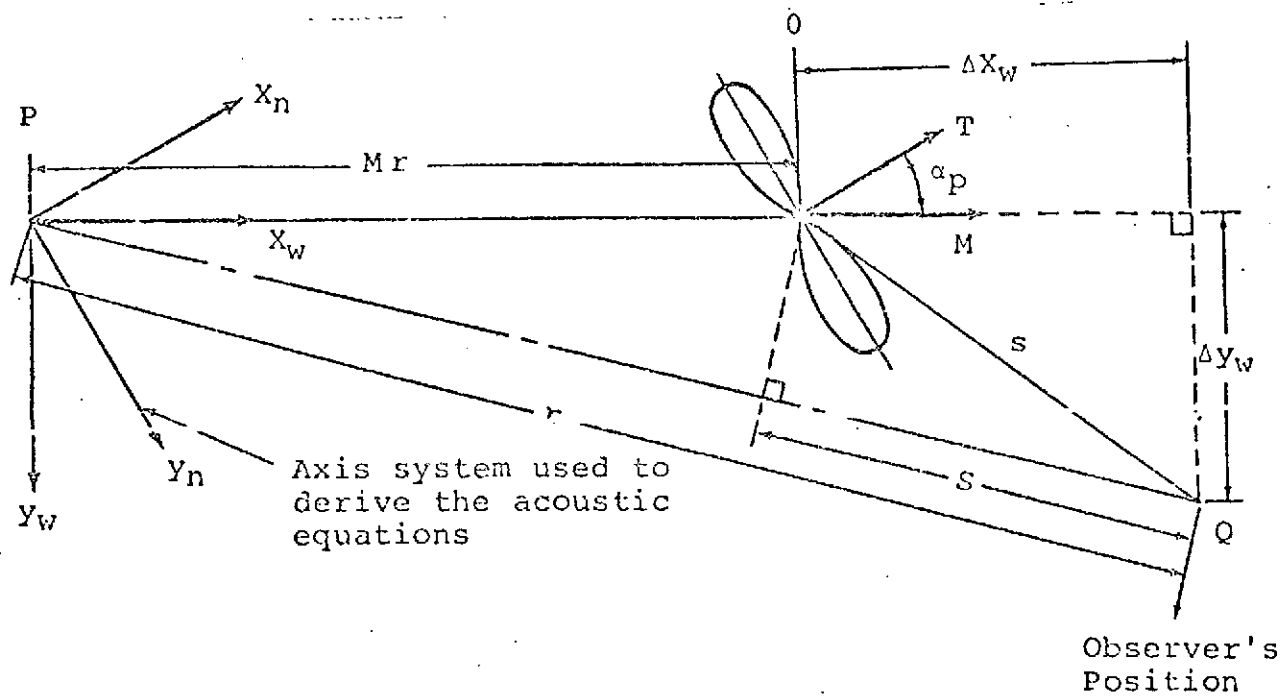
Figure 3. Relationship between Rotor Orientation, Free stream Velocity and Far-Field Observer

15

while
$$S = \sqrt{\Delta X_W^2 + \beta^2 (\Delta Y_W^2 + Z_W^2)} \qquad (\text{II-9})$$
$$\beta^2 = 1 - M^2 \qquad (\text{II-10})$$

The variable $Z_n \equiv Z_W$ has been introduced to allow the observation point to be moved to specified "side-line" positions. A derivation of eqs. (II-6) through (II-10) is presented in detail in ref. 4 .

Eqs. (II-1) through (II-10) predict the rotational noise of the rotor craft for specified flight conditions and corresponding values of the harmonic force coefficients. A method of specifying the harmonic force coefficients is presented in the next subsection.

Aerodynamic loading laws of the rotor: It has been established by many authors that blade loading harmonic data is important in being able to predict rotational noise of a helicopter. Unfortunately, adequate theoretical prediction techniques and/or sufficiently reliable experimental data to quantitatively define the higher loading harmonics is lacking at the present time. To surmount this difficulty for the helicopter, Lowson & Ollerhead (ref. 1) developed the concept of a "rotor loading law." They hypothesized that the higher harmonic airloads decrease by some power of the harmonic number. This exponent is referred to as the "loading law" and is designated by the symbol "n".

By empirically fitting airload data of helicopters in
level steady-state flight, a numerical value of 2 was
thought to be representative. If the phase of the
loading harmonics is assumed to be random, the follow-
ing expression results:

$$F = F_{steady} / \lambda^{(n+0.5)}$$

where $n = 2.0$

$F = $ harmonic airloads

$\lambda = $ loading harmonic number

It is assumed that the higher harmonic airloads of
thrust, drag, and radial force all obey the same
loading law.

Thus,

$$C_{\lambda T} = C_{OT} / \lambda^{(n+0.5)} \qquad\qquad (II-11)$$

$$C_{\lambda D} = C_{OD} / \lambda^{(n+0.5)} \qquad\qquad (II-12)$$

$$C_{\lambda C} = C_{OC} / \lambda^{(n+0.5)} \qquad\qquad (II-13)$$

where $n = 2.0$.

If eqs. (II-11), (II-12), and (II-13) are sub-
stituted in eqs. (II-1) through (II-10), the
rotational noise generated by a helicopter in level
steady-state flight is completely determined.
The loading law concept simplifies much of the mathe-
matics involved in the analytical description of a
rotor's operating state. The purpose of the measure-

ment program described in the next report section is
to show that measured values of the loading law expon-
ent do yield a close correlation with measured acoustic
rotational spectra under several different rotor
operating conditions.

III.   WIND TUNNEL MEASUREMENTS

This section of the report describes the procedures
used to obtain blade surface pressure and acoustic
noise data from a model rotor. It includes a descrip-
tion of the wind tunnel model, general test procedures
and measurement techniques, the test conditions, blade
pressure and acoustic instrumentation, and data
analysis techniques. This effort was conducted to
check out the accuracy of a basic formulation repre-
senting rotor rotational noise in non-axial flight.
Testing was conducted as an addendum to the Reference
8 experimental program to take advantage of concurrent
aircraft model wind tunnel testing, and represents
a portion of that effort expended to develop a better
noise prediction capability.

OBJECTIVE AND TEST PROCEDURES

The specific technical objective of the measurement
program was to extend and verify the proposed method

of rotational noise prediction for rotors in non-axial flight. Specifically, the influence of rotor operating conditions, such as disc angle of attack and inflow, on the blade airload harmonic decay laws and its relationship to acoustic harmonics was sought.

The test program was conducted in the Boeing Vertol V/STOL Wind Tunnel which is a closed-circuit, single-return type with a rectangular test section of 20 x 20 feet in cross-section operated in the solid walls configuration. The dynamic rotor test stand used during this model test was sting-mounted for both hover and forward flight testing. The model itself consisted of an extensively instrumented three-bladed model rotor, geometrically scaled to represent 1/7.5 scale production CH-47B blades with constant chord and linear spanwise twist. The airfoil·section used was the Vertol 23010-1.58. Absolute pressure transducers, located at the 75-percent radial station, were used to measure blade element airloads on the upper and lower blade surfaces. In addition, four microphones were placed upstream of the model on the advancing rotor blade side to record the acoustical noise generated by the rotor at several operating conditions. Data was obtained during the test program during hover

and forward flight. For hover, which was conducted at a tip speed of 250 feet per second, the model was tilted forward into the airstream to an angle of 45 degrees while collective pitch sweeps were made in approximately two degree increments. Testing in forward flight consisted of setting a collective pitch and varying the rotor shaft angle. The conditions analyzed in detail in this report consisted of a tip speed of 250 feet per second for an advance ratio of 0.15, and a tip speed of 500 feet per second for an advance ratio of 0.35.

ROTOR BLADE SURFACE PRESSURE DATA

The pressure transducers used in the test program were mounted at the 75-percent radius on the top and bottom surfaces of one of the three model rotor blades. The sensing surface of the transducers was set even with the outer surface of the blade by mounting the trans- ducer itself slightly below the airfoil surface. Thus, a smooth, properly contoured air-foil surface could be maintained. The transducers consisted of Kulite LPL-125-5 semi-conductor diaphragm sensors, one-eighth inch in diameter with a pressure range of 0 to 25 psia, a dynamic range of up to 60 decibels, a frequency response in excess of 20,000 Hz, and a linear response to pressure throughout the range of

interest. They were mounted on an elastomeric
sandwich with additional vibration isolation provided
for to minimize strain and acceleration effects. A
screen was placed over the diaphragm to protect the
sensor from foreign object damage. Wiring from the
transducer to the slipring assembly on the rotor
shaft was routed internally to the blade to maintain
a smooth airfoil surface.

Data signals from the pressure transducers were fed to
signal conditioners which provided for amplification
and filtering of each data channel. This conditioned
analog data was supplied to data multiplexers con-
taining analog-to-digital convertors which transformed
the data to digital format. Approximately two seconds
worth of data from each stabilized data point was then
sent through an IBM 1800 data processor which then
permitted the storage of this raw digital data on tape
along with pertinent rotor model and wind tunnel para-
meters. This stored digital data was next transferred
to an IBM 360 computer for further processing. This
involved converting the pressure data to engineering
units, scanning the time-history data to edit out
non-repeatable events, averaging several rotor
revolution cycles to get a statistically more meaning-
ful data picture, and applying the appropriate trans-

ducer and   instrumentation correction factors.

Typical data format at this stage consisted of chord-wise pressure distributions at various rotor blade azimuth positions as illustrated in figure 4 taken from reference 8 in which additional details of the pressure measurement procedures are contained.

In order to make use of the blade loading data in a form suitable for incorporation in the rotational noise formulation described in Section II of this report, the pressure data was harmonically analyzed after chordwise integration. The magnitudes of the forces acting on the top and bottom surfaces of the blade at the 75 percent radius were converted to a differential value whose logarithm to base 10 was then plotted as a function of the logarithm (base 10) of the load harmonic number. This format (see figure 8) permits the establishment of a least-square line through the blade load data whose slope represents the exponent "n" in the blade loading law.

ROTOR ROTATIONAL NOISE DATA

The acoustic data from the model rotor was measured with four Bruel and Kjaer Model 4133 microphones located upstream from the model on the advancing blade side (figure 5). These transducers consisted of
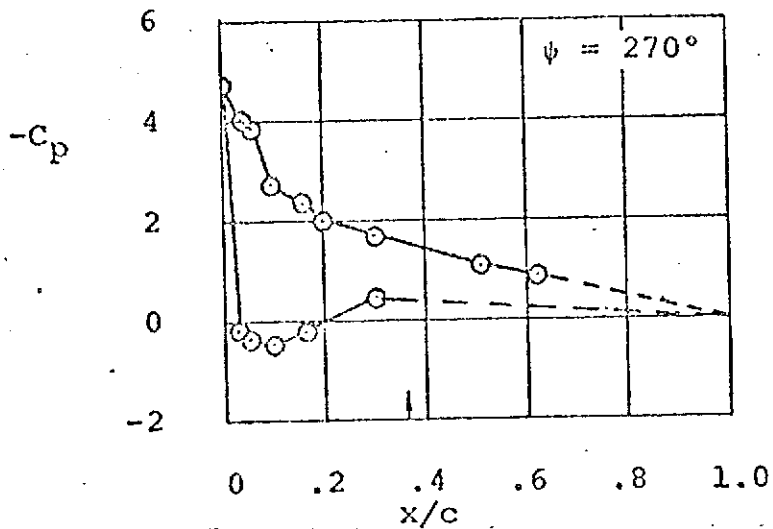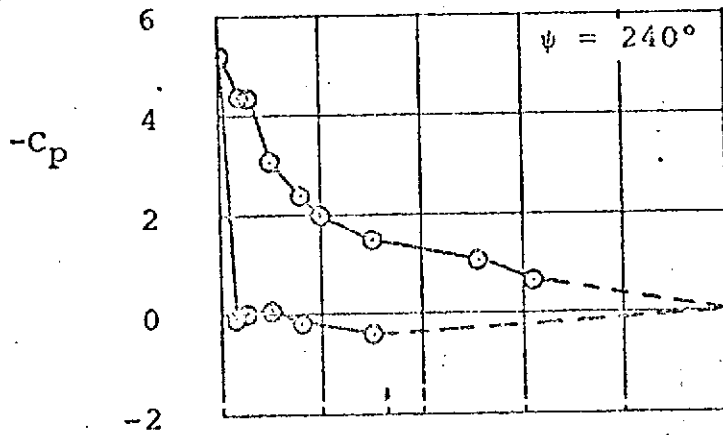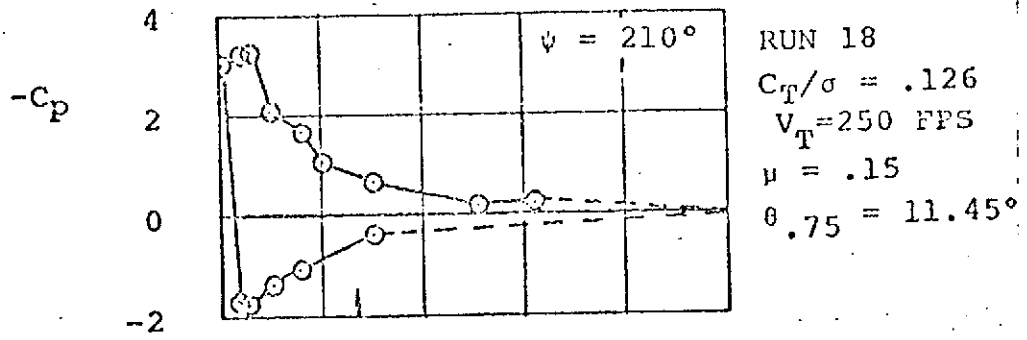
Figure 4. Chord-wise Pressure Distributions

PLAN VIEW

FLOW ⟶
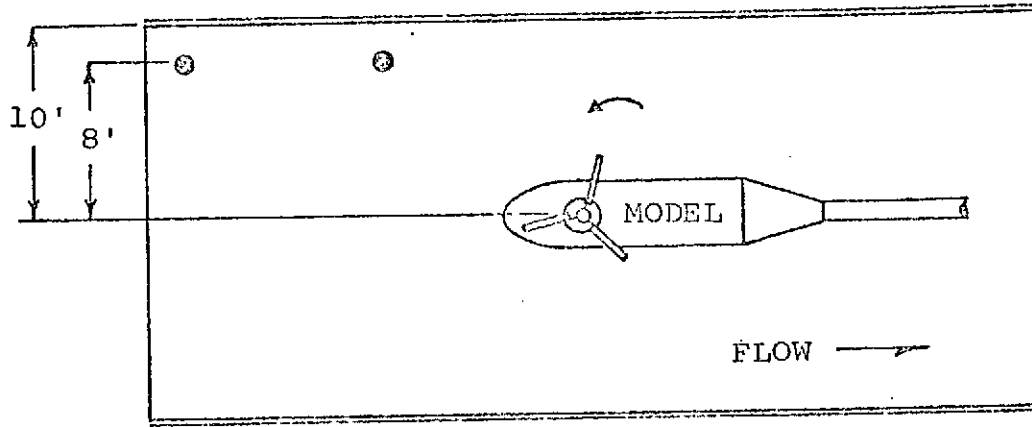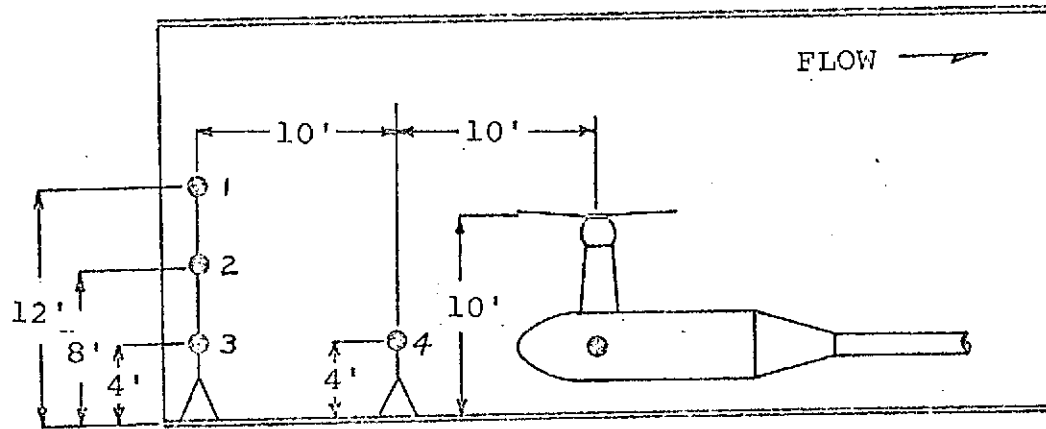
ELEVATION VIEW

FLOW ⟶

Figure 5. Microphone Locations for Model Rotor
Noise Measurements

one-half inch diameter condenser microphones with signal conditioning equipment to optimize the signal to noise ratio during recording. Thirty to fourty second acoustic data records were taken during each stabilized model data point coinciding in time with the recording of the blade pressure data. The analog signal from each of the four microphones was recorded in the FM mode on an Ampex SP-300 tape recorder. The entire acoustical instrumentation system was determined to be essentially flat in frequency response from 20 Hz to 3000 Hz as determined by laboratory calibrations. Microphone sensitivity to rotational noise was enhanced through the use of nose cones to reduce excessive wind noise in forward flight. Correlation of the acoustic data with blade pressure data recorded on an independent system was assured by recording a rotor one-per-rev signal and voice commentary on auxiliary channels of the acoustic data recorder. The placement of the acoustic transducers was determined by several factors. One of these was that the transducer location should coincide with a location in the tunnel surveyed to define the reverberent effects introduced by the wind tunnel test section itself. A second requirement, to satisfy acoustical theory, was met by locating the microphones at least

one and one-half to two rotor diameters away from
the model center of rotation. The third major require-
ment was that the microphone and its supporting
structure should not interfere with the rotor aero-
dynamic flow.

The tape recorded acoustic data was subjected to a
narrow-band frequency analysis using a Federal
Scientific Model UA-6 spectrum analyzer. A 2 Hz filter
bandwidth was employed to distinguish between the
harmonics of rotational noise in the frequency range
of 0Hz to 1000 Hz . Initial analyses indicated that
spectral levels fluctuated randomly in amplitude as a
function of time, making the determination of a mean
harmonic sound pressure level difficult. The causes
of these fluctuations are the random loads imposed on
the rotor due to local small-scale turbulence in hover
and interfering wind noise over the microphone trans-
ducer in forward flight. For this reason, a second
analyzer, the Federal Scientific Model 129H, was used
to ensemble average a 32 second sample of acoustic
noise, which represented 64 statistically independent
spectra. The latter process enhanced the identifica-
tion and precision of the rotational noise harmonic
levels considerably, as illustrated in Figure 6 .

RUN 28 $\mu = .35$ $V_{TIP} = 500$ FPS.

THRUST = 253. LBS.
DATA POINT 12   SHAFT ANGLE = -3°

SOUND PRESSURE LEVEL

100

RAW DATA

10 dB

0   .2   .4   KHz   .6   .8   1.0

FREQUENCY

THRUST = 253. LBS.
DATA POINT 12   SHAFT ANGLE = -3°

SOUND PRESSURE LEVEL

100

ENSEMBLE
AVERAGED DATA

10 dB

0   .2   .4   KHz   .6   .8   1.0
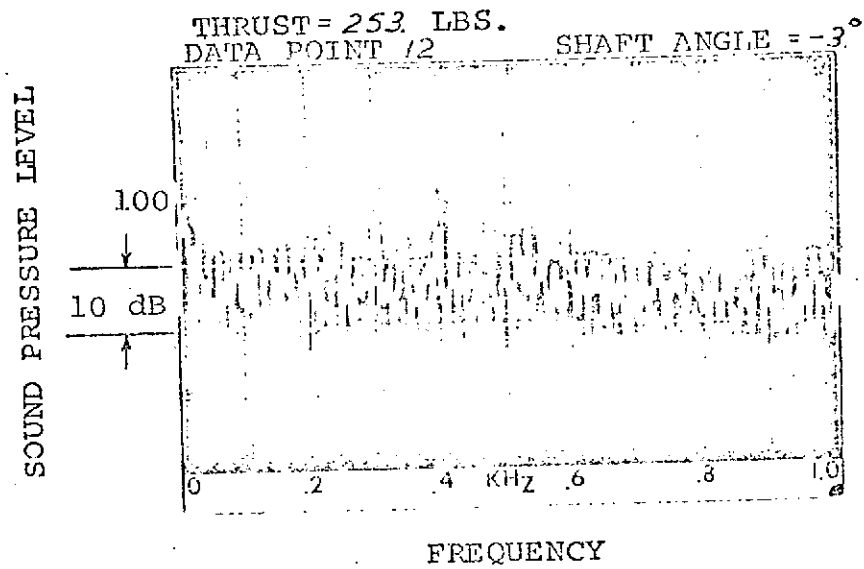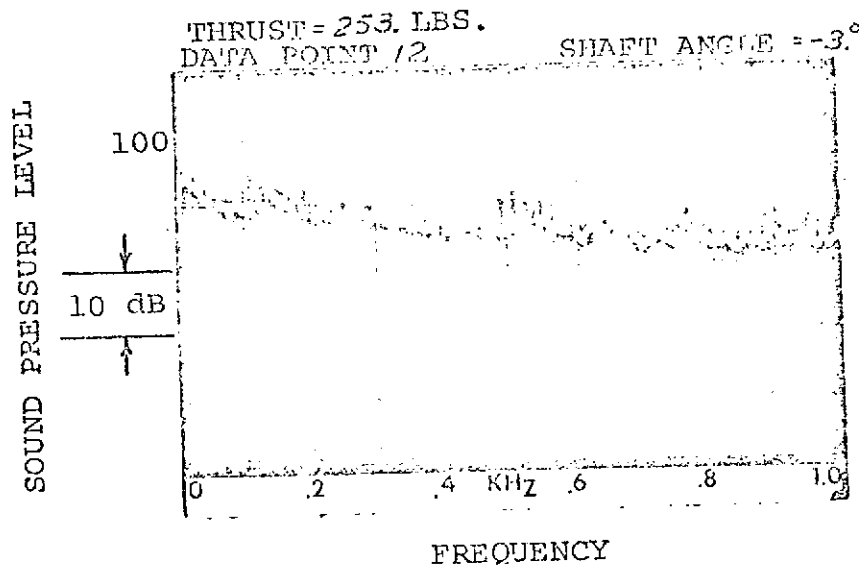
FREQUENCY

Figure 6.   Effect of Signal to Noise Ratio Enhancement
by Ensemble Averaging

27

Non-linearities in the acoustic data were handled as
follows. First, electrical frequency response calibra-
tions were conducted prior to the test on the entire
data recording and analyses system. Figure 7-a
illustrates a typical data track calibration.
Deviations from the amplitude response with respect
to the response at the calibration test frequency
(250 Hz), used at the time of the model test, were
applied to the data from the frequency analyzer. The
second, and major, correction applied to the data arose
from the fact that the tunnel test enclosure added a
substantial amount of noise to the data in the form
of reverberations. To ascertain the magnitude of these
non-linearities, a wind tunnel noise survey was con-
ducted prior to the model tests at various locations
within the tunnel test section (ref. 9). The results
of that survey indicated that the measured level in the
tunnel enclosure is very frequency dependent and
fluctuates generally between five and twenty decibels
above the level of a noise source measured out-of-
doors (Figure   7-b). The curve shown is derived
from reverberation calibrations using a random noise
source and analyzed in 2 Hz wide filter increments to
correspond to the bandwidth used for the model rotor

28

a. Acoustic Data System Electrical Response
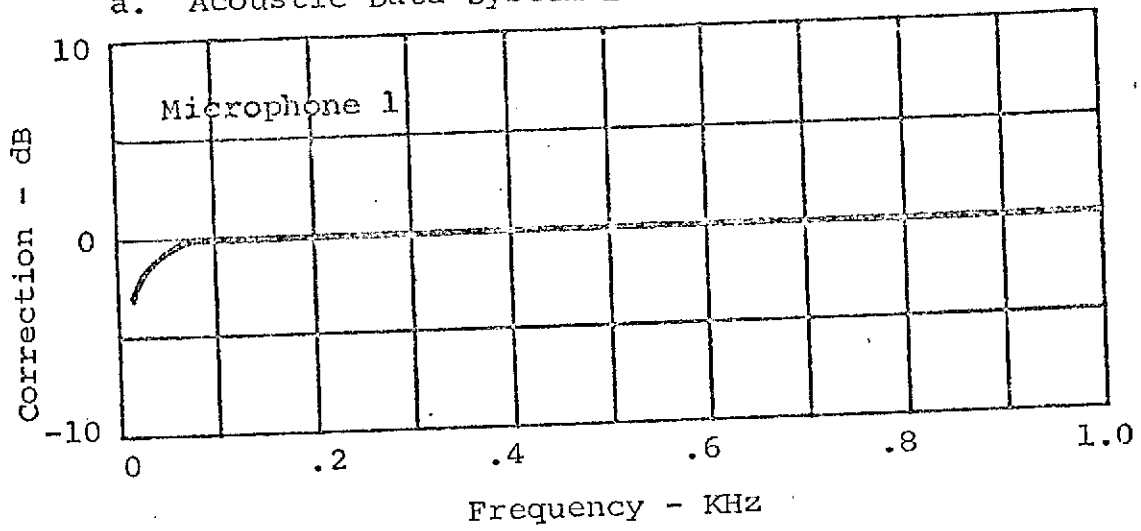
Frequency – KHz

b. Tunnel Test Section Reverberant Response
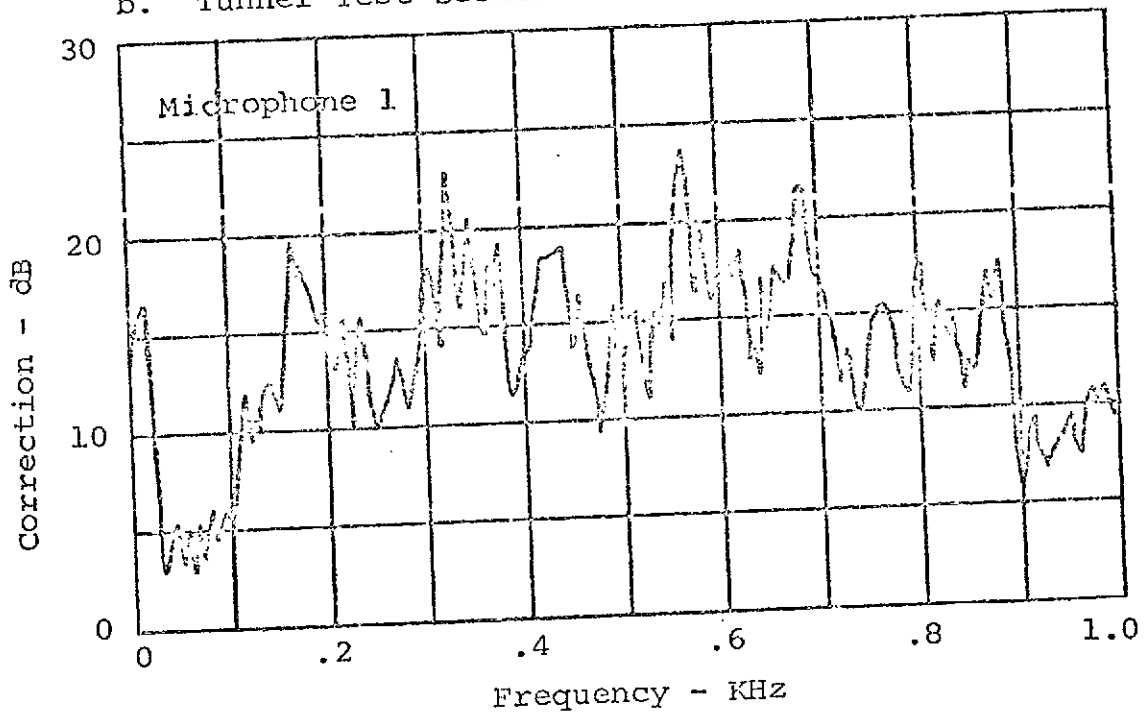
Frequency – KHz

Figure 7.   Correction Factors for Acoustic Data
            Non-Linearities

29

noise analyses. Since the modified acoustic theory predicts rotor harmonic sound pressure levels, the frequency analyzed measured data was prepared in a format which readily invites comparisons. Both the predicted and the measured rotor harmonic data, after correcting for electronic and reverberation non-linearities, are therefore presented in terms of sound pressure level as a function of noise harmonic number in the following report section dealing with correlation of theory and measured data.

IV. TEST RESULTS AND CORRELATION WITH THEORY

This report section details the results of the blade pressure and rotational noise measurements. Corrected data are presented in quantitative graphic format to facilitate comparison of the acoustic measurements and theoretical noise predictions. The latter are derived from the pressure data presented immediately preceeding the corresponding harmonic noise data. This format also permits a qualitative assessment of the scatter and precision of both measured quantities.

Two theoretical noise prediction lines are indicated on each plot. The solid line represents the harmonic sound pressure levels which result from using the

harmonic pressure slope indicated by a solid line on
the pressure data. A high pressure slope, or loading
law constant "n"; results in a low harmonic noise
prediction. Conversely, a low pressure slope yields
a high harmonic noise prediction as indicated by the
dashed lines. This range of noise prediction results
from assigning a range of probable least square lines
through the pressure data derived by considering
several factors. One of these is that the sixth pres-
sure harmonic was omitted in deriving a least square
fit in those data runs where the rpm of the rotor
was low. This criteria seemed reasonable upon examina-
tion of the influence of a rotor mechanical interaction
which resulted in considerably higher values of this
harmonic than could reasonably be expected. The same
type of reasoning was applied when omitting the first
harmonic of the pressure data in certain cases when its
value appeared low due to a rotor control input. The
magnitude of the measured steady pressure, indicated
by a "plus" symbol, has been used instead on occasion
to compensate for this and when its inclusion in
deriving a least square line seemed warranted in view
of the general data scatter. In addition to the above
criteria, high harmonics of pressure above the tenth, or

pressure harmonics which fell fifty to sixty decibels below the value of the steady pressure, were selectively omitted due to dynamic range limitations of the pressure instrumentation.

Run and Data Point numbers on the referenced figures are in keeping with the format established in reference 8 . Microphone position numbers are as indicated in figure 5 of this report. Rotor shaft angle notation is such that negative values indicate an inclination into the airstream, measured from the vertical.

HOVER

The model rotor shaft angle for all hover data points was kept at (-45) degrees to permit the downwash to flow clear of the tunnel test section without recirculating through the rotor.

Advance Ratio = 0; Tip Speed = 250 ft/sec: The results of hover testing are indicated in Figures 8 through 12 . Figure 8 is data from Run 26, Data Point 2 for microphone positions number 1 through 4. Except for noise harmonic numbers six and fourteen, correlation with theory is excellent at position 1, even at this low thrust of three pounds. Microphone positions 2 and 3 exhibit similar good correlation with several harmonics being high for position 2 and low for

32
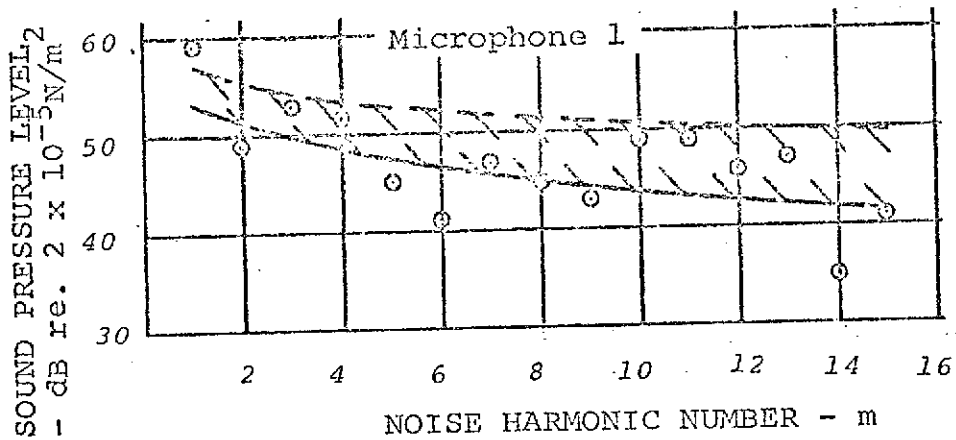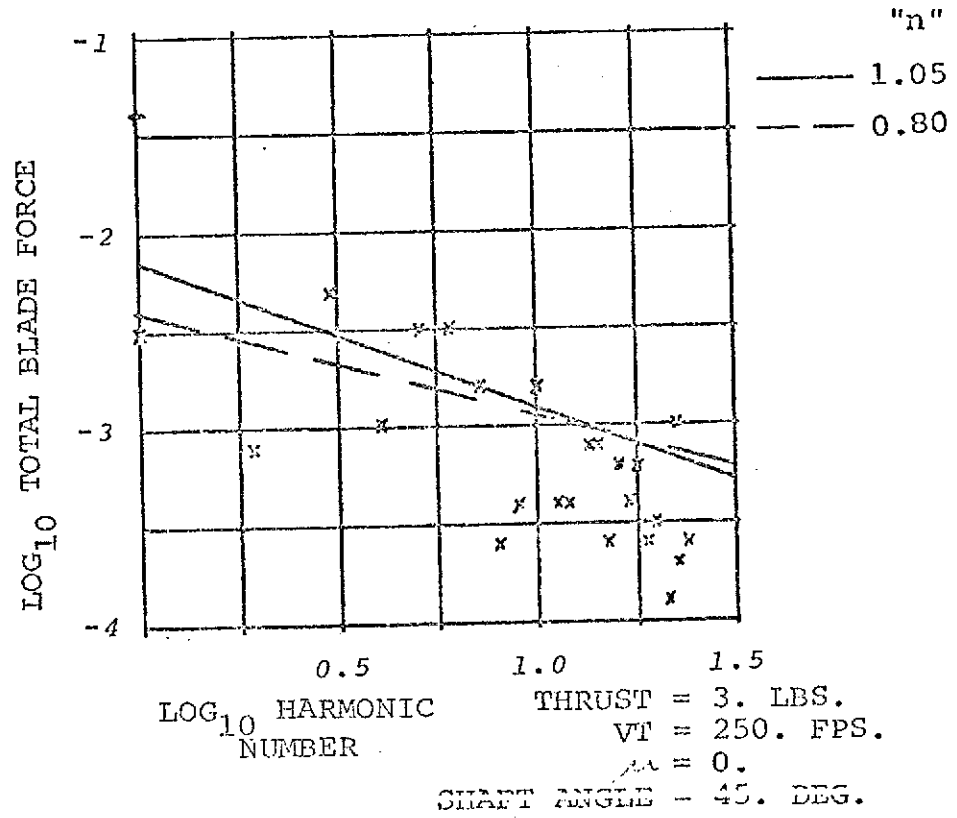
Figure 8.   Correlation Results for Hover Run 26
Data Point 2
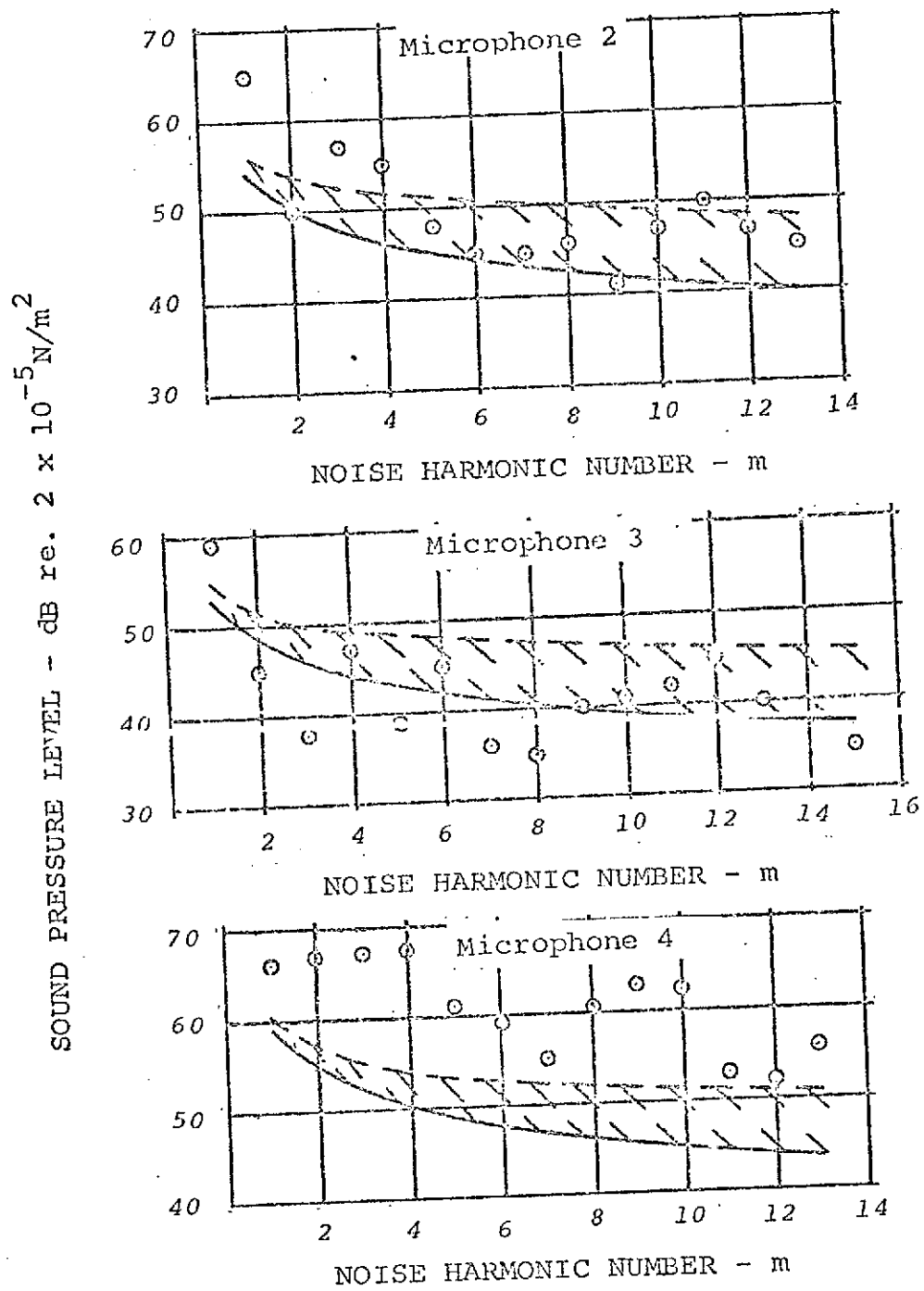
Figure 8. Concluded

position 3. Correlation of noise theory with micro-

phone position 4 data is not as good, with the theory

underpredicting the measured data by a moderate amount.

Overall correlation with theory is very good consider-

ing the amount of scatter exhibited by the pressure

data.

Figure 9 represents measured pressure data and

measured and predicted noise data for Run 26, Data

Point 4. Rotor thrust is 18 pounds. Except at micro-

phone position 4, correlation with theory is not good.

The same conclusion is derived by comparing data from

Run 26, Data Points 5 and 7 (Figures 10 and 11 ,

respectively). There is considerably more scatter in

the acoustic data in these last four data points com-

pared to Data Point 2, even though the scatter in the

pressure harmonic data is similar. It is interesting

to note, however, that correlation would have improved

considerably by forcing the pressure harmonic decay

lines through the steady pressure data point. This

would not explain the considerable amount of scatter

exhibited by the measured noise data, though.

In view of the poor correlation shown for Data Points

4, 5 and 7, no further correlation with theory was

attempted. The data from Data Point 2, however, was
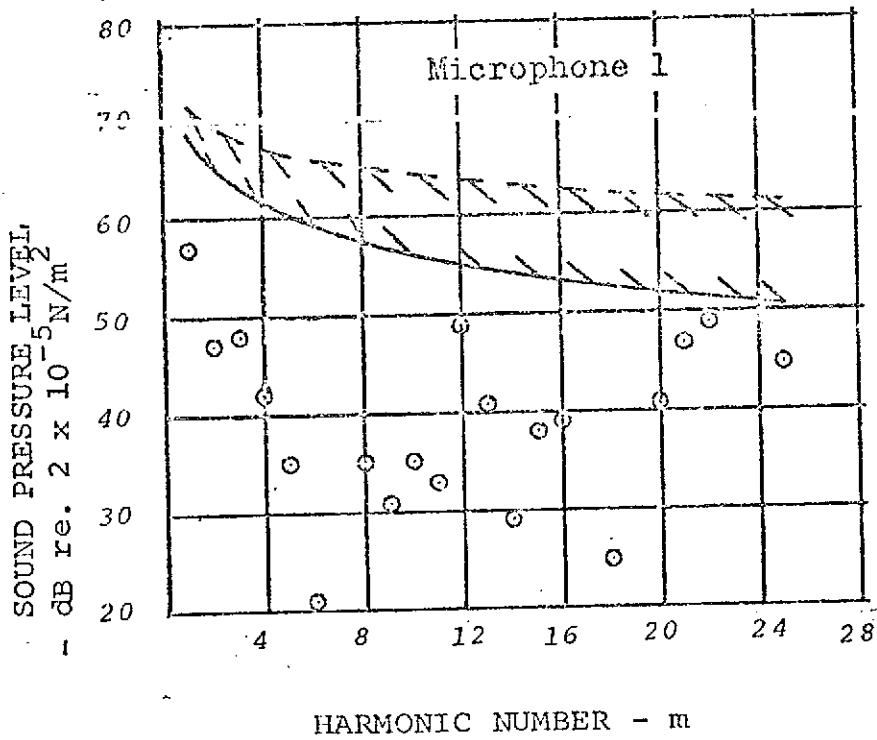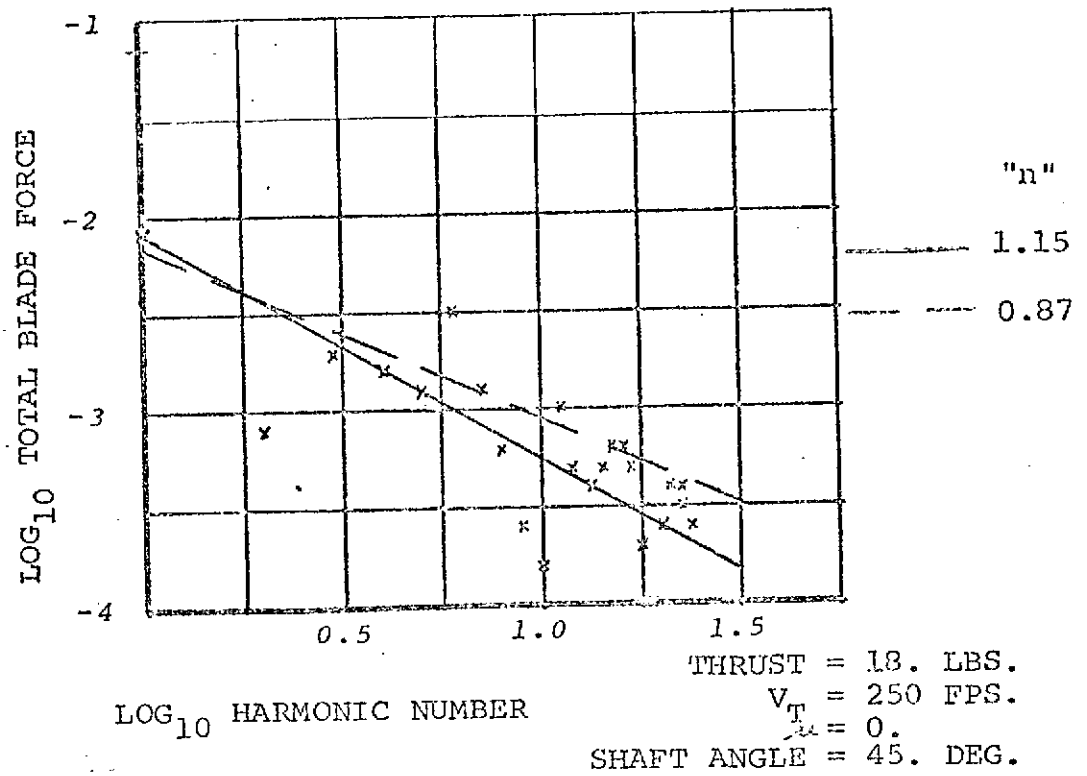
Figure 9. Correlation Results for Hover Run 26
Data Point 4
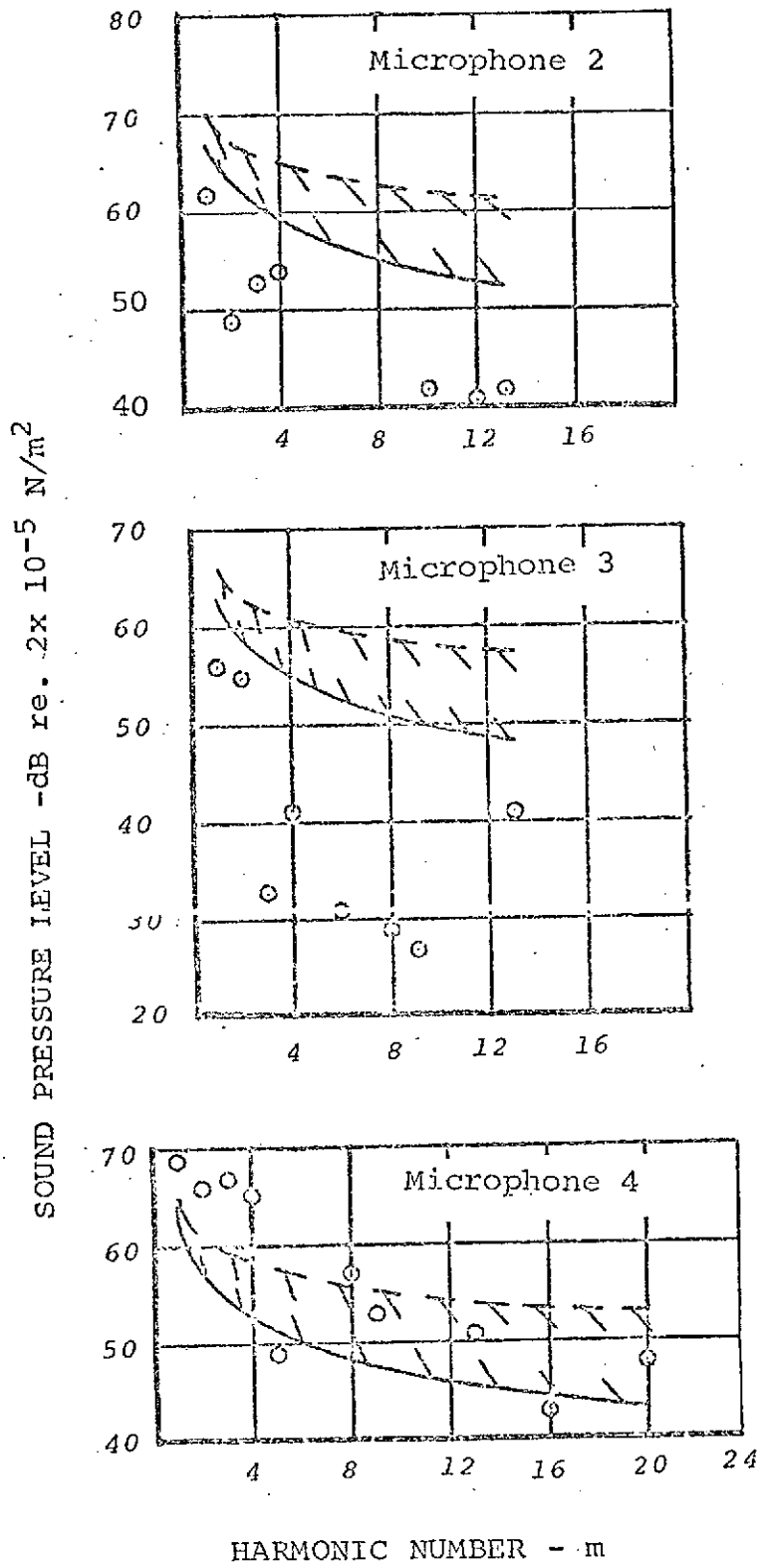
Figure 9. Concluded
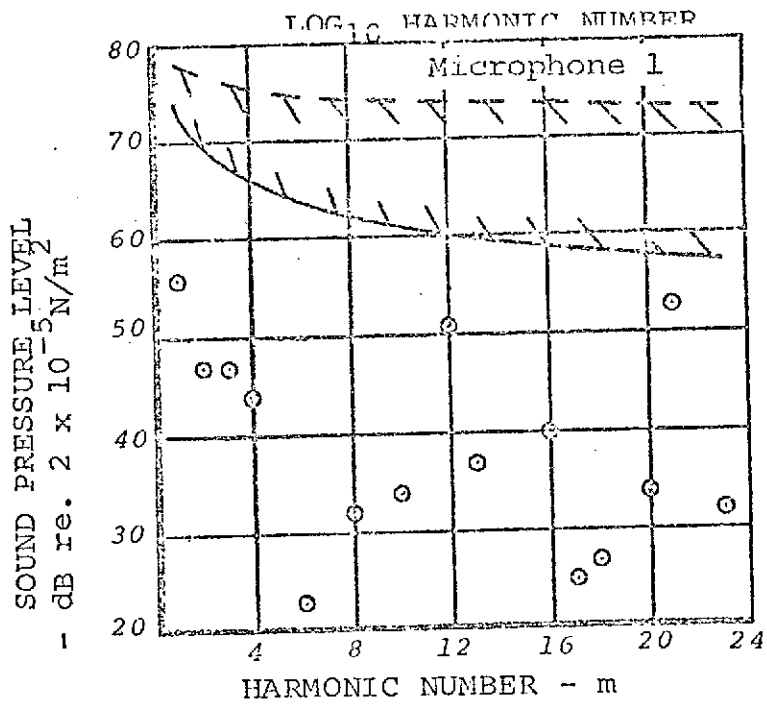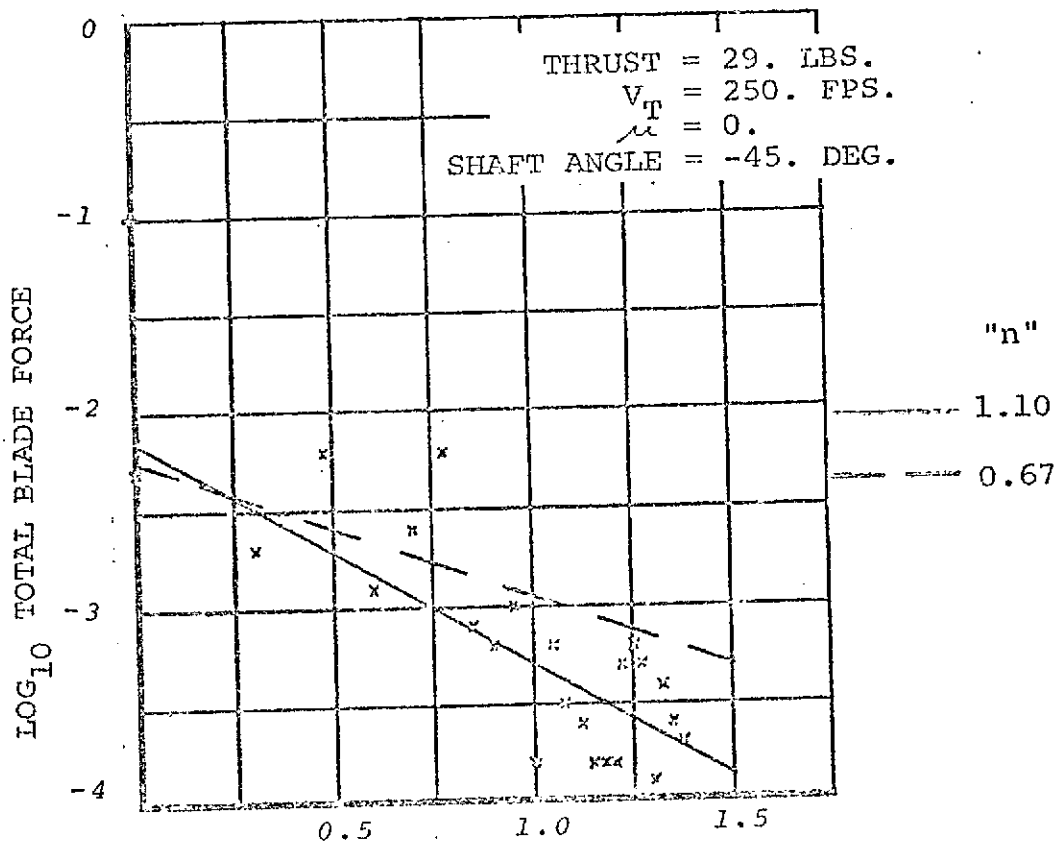
Figure 10. Correlation Results for Hover Run 26
Data Point 5
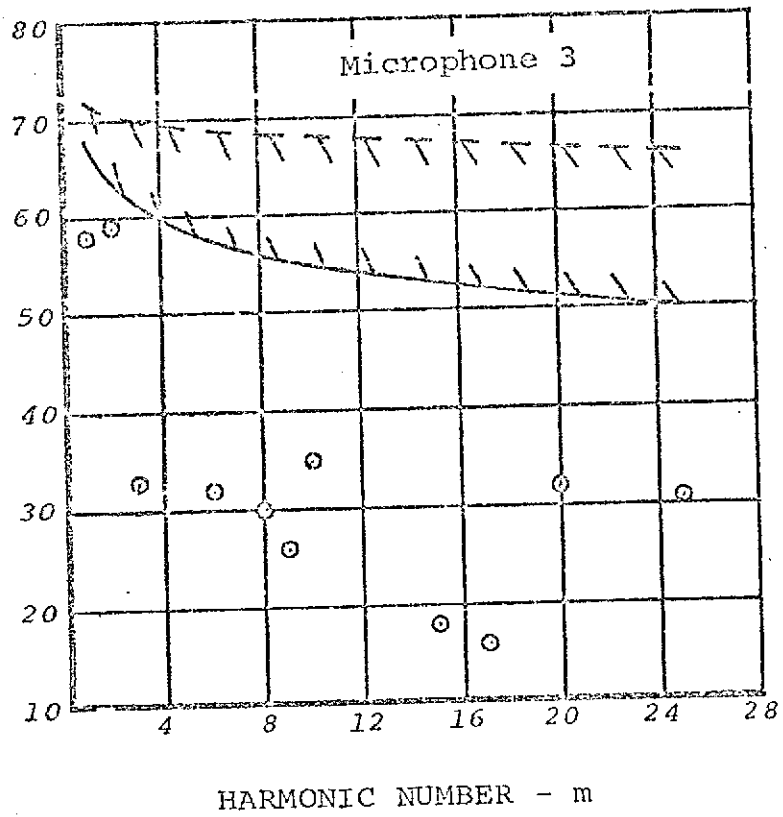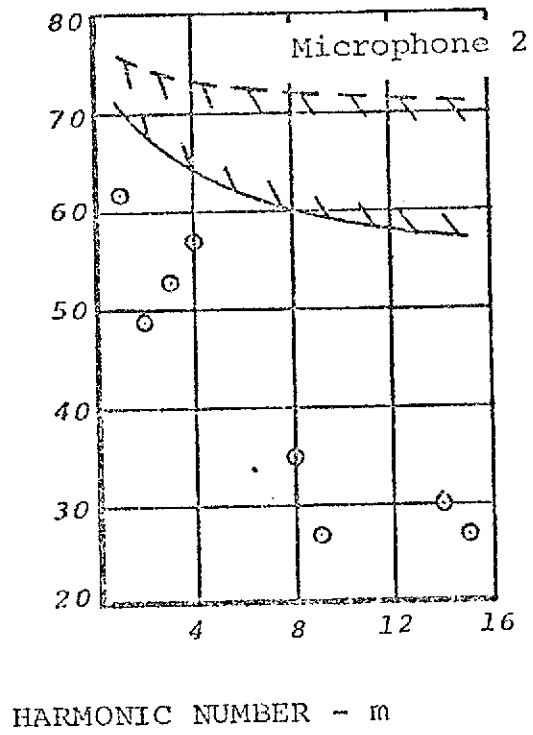
Figure 10. Continued
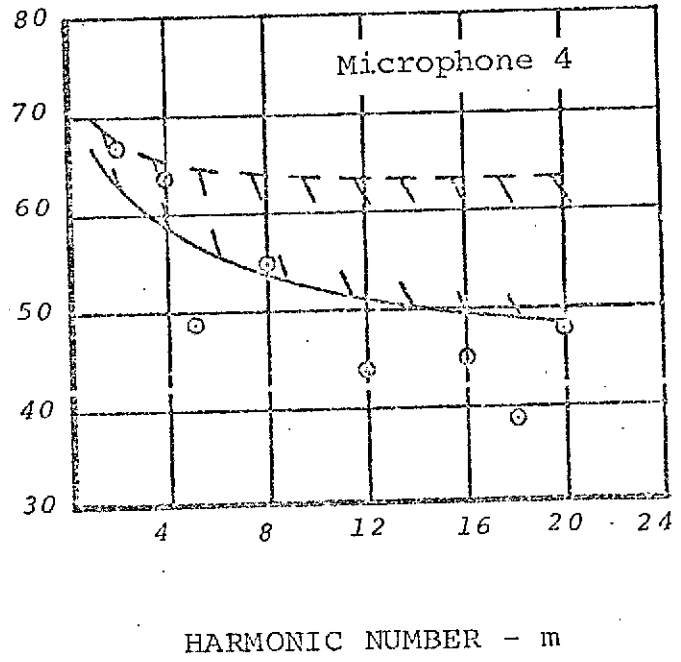
Figure 10. Concluded
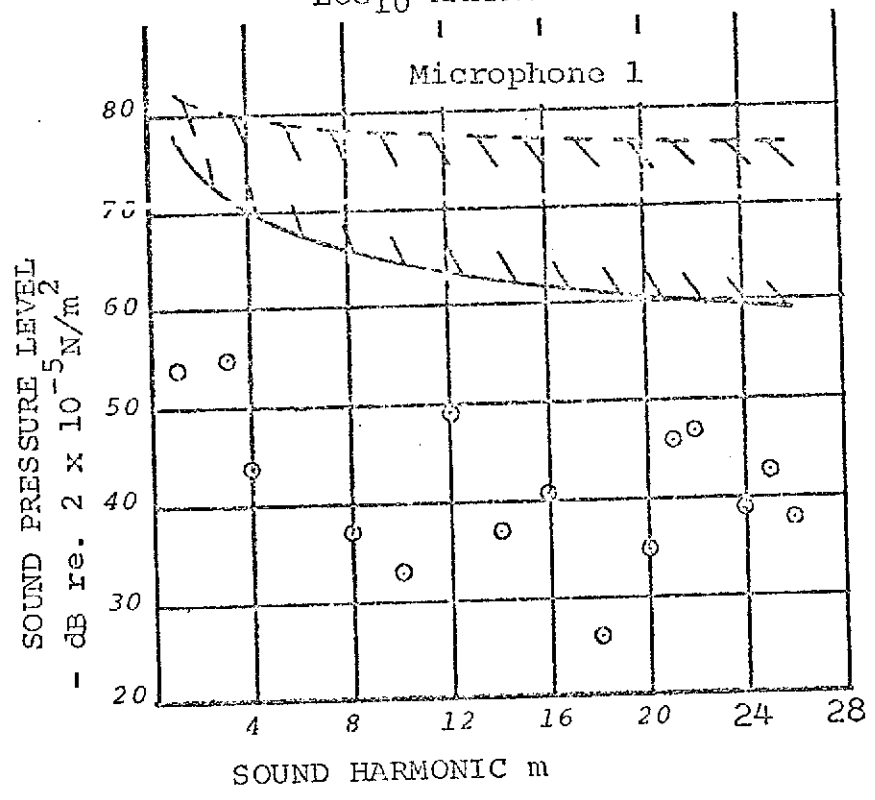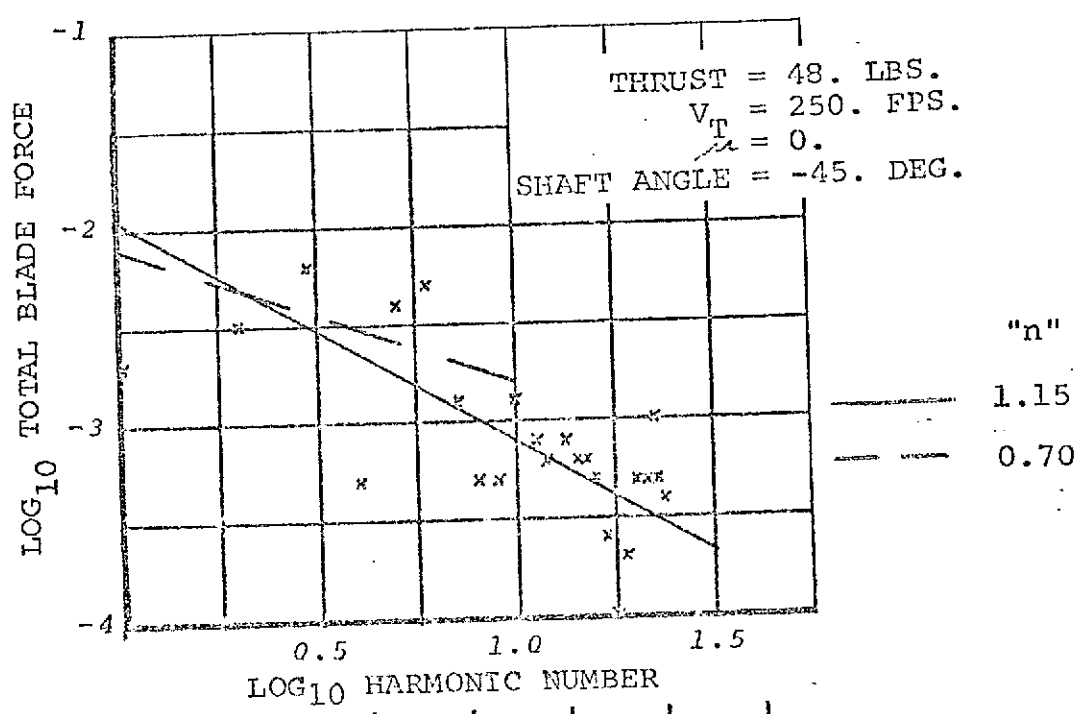
Figure 11.   Correlation Results for Hover Run 26
Data Point 7

41
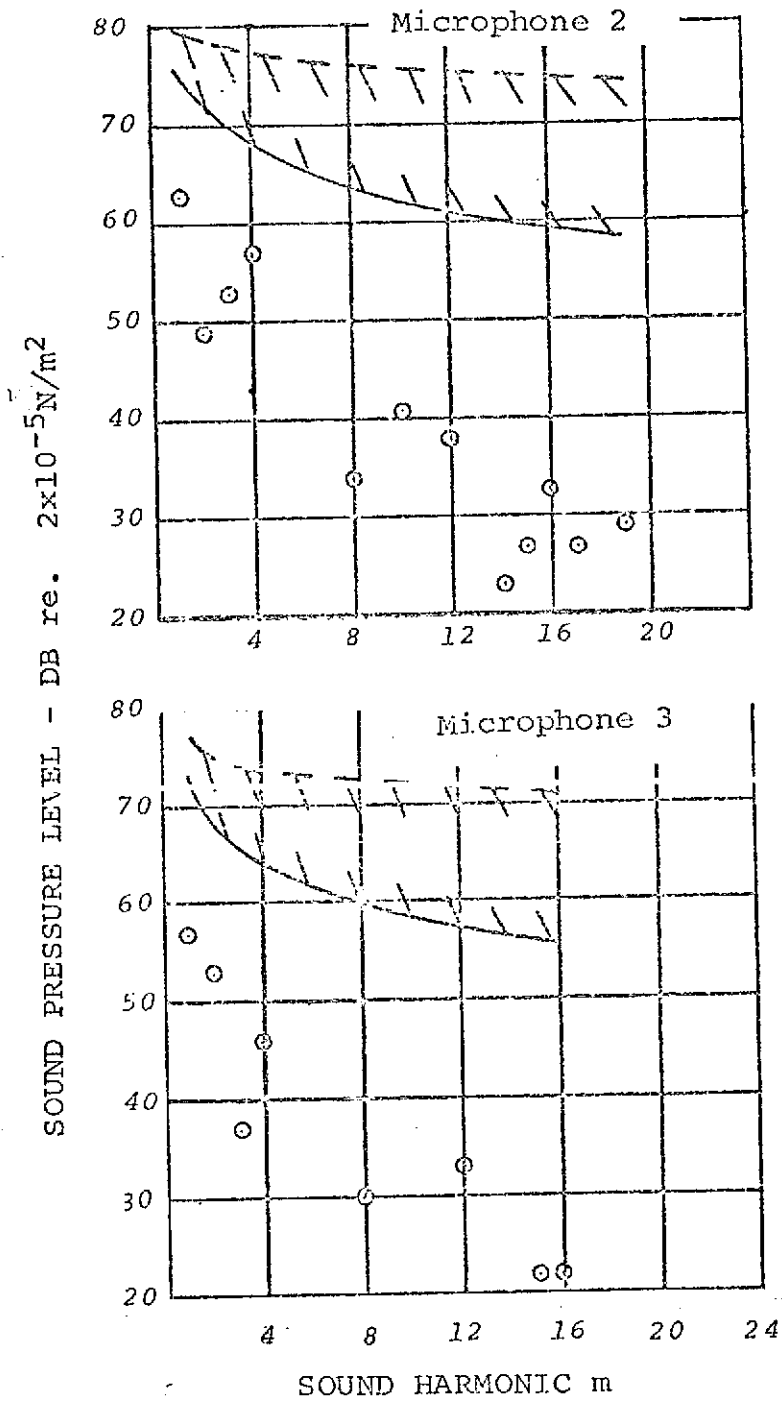
Figure 11. Continued

42

Microphone 4
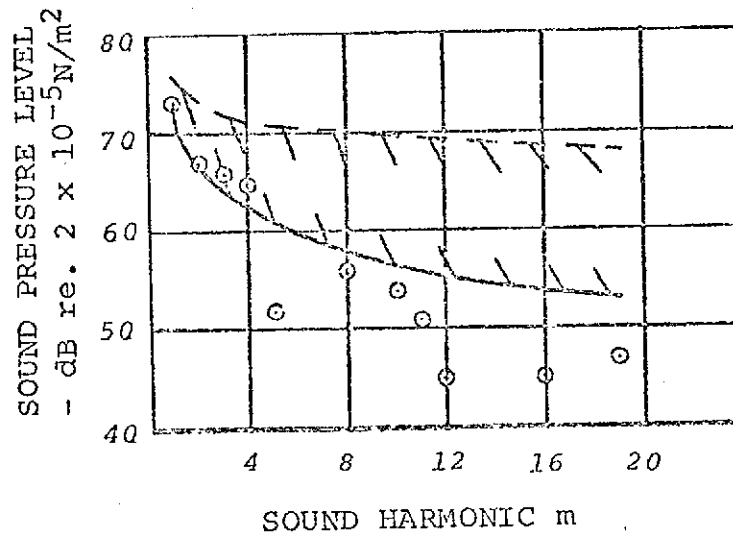
Figure 11. Concluded.

re-analyzed in terms of the rotor's directivity.

Figure 12 indicates the directivity characteristics of certain rotational noise harmonics in a vertical plane through the model rotor. Only those measured noise harmonics which yield a definitive pattern have been illustrated to show the moderate degree of correlation with theory. The measured noise lobes are more pronounced than the theory would indicate.

FORWARD FLIGHT

Two forward flight speeds resulting in varying acoustic spectra have been investigated. Rotor collective pitch was set at a fixed value and the rotor shaft angle varied.

Advance Ratio = 0.15; Tip Speed = 250 ft/sec: Figures 13 through 15 summarize the results of the low speed forward flight pressure and acoustic measurements on the model rotor. Figure 13 is for Run 18, Data Point 8 and Microphone Position 1. Again, there is considerable scatter in the pressure data resulting in fairly wide noise prediction limits.

Even so, the measured acoustic data falls below the predicted levels.

Data Point 9 of Run 28 also exhibits considerable pressure and acoustic data scatter (see Figure 14).
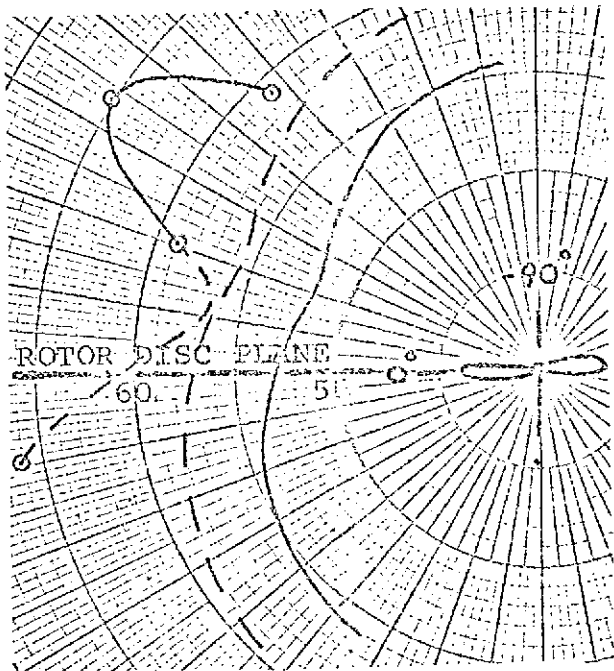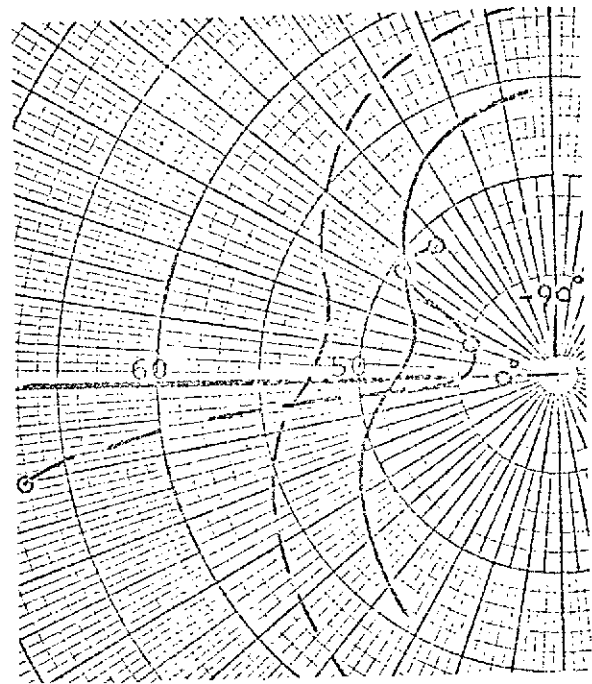
SOUND HARMONIC   m = 1   m = 2

NOTE: NUMBERS ALONG ROTOR DISC PLANE INDICATE
        SOUND PRESSURE LEVEL IN DECIBELS
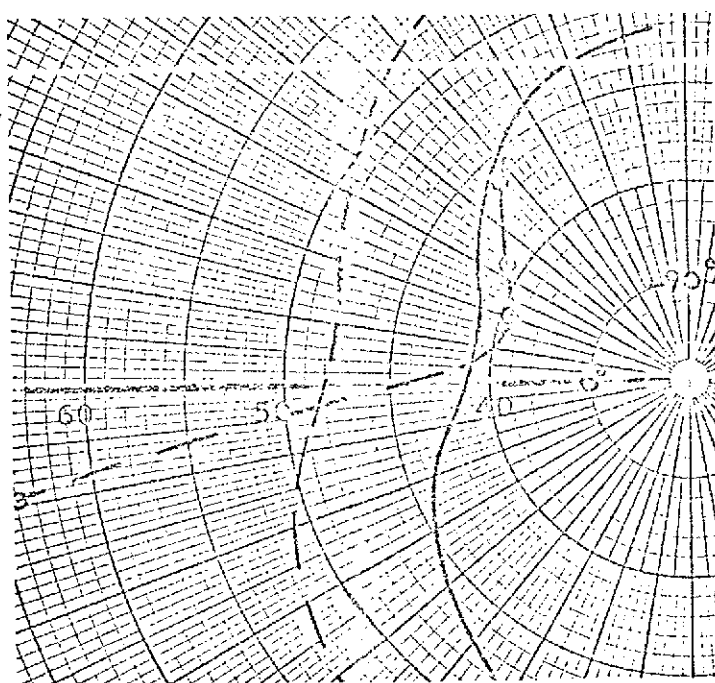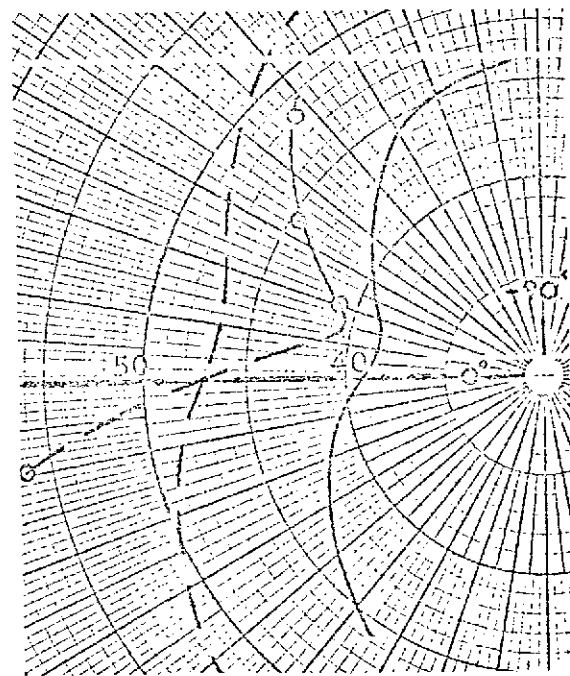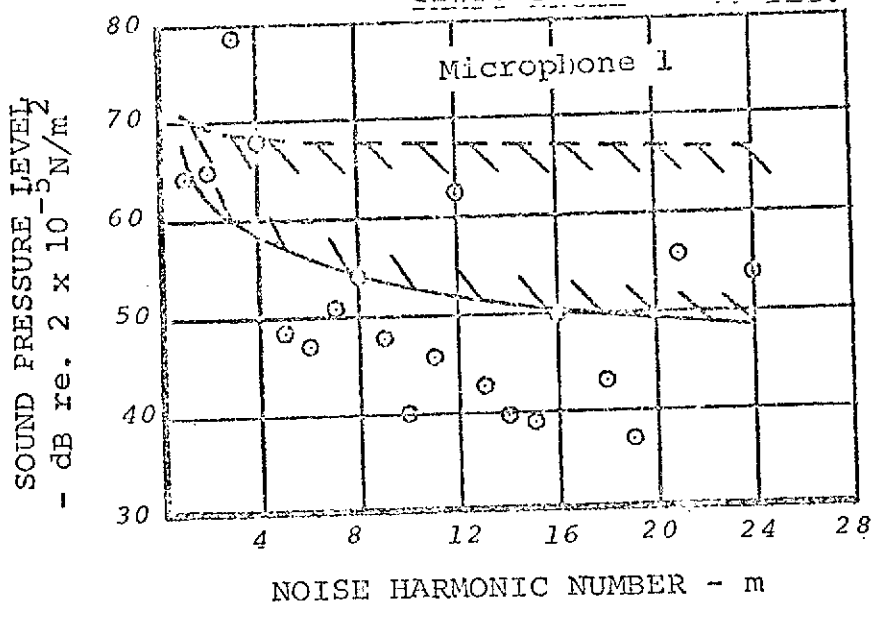
m = 9   m = 13

"n"
——— 1.05
−−− 0.80

Figure 12.   Directivity of Model Rotor for Hover
             Run 26 Data Point 2
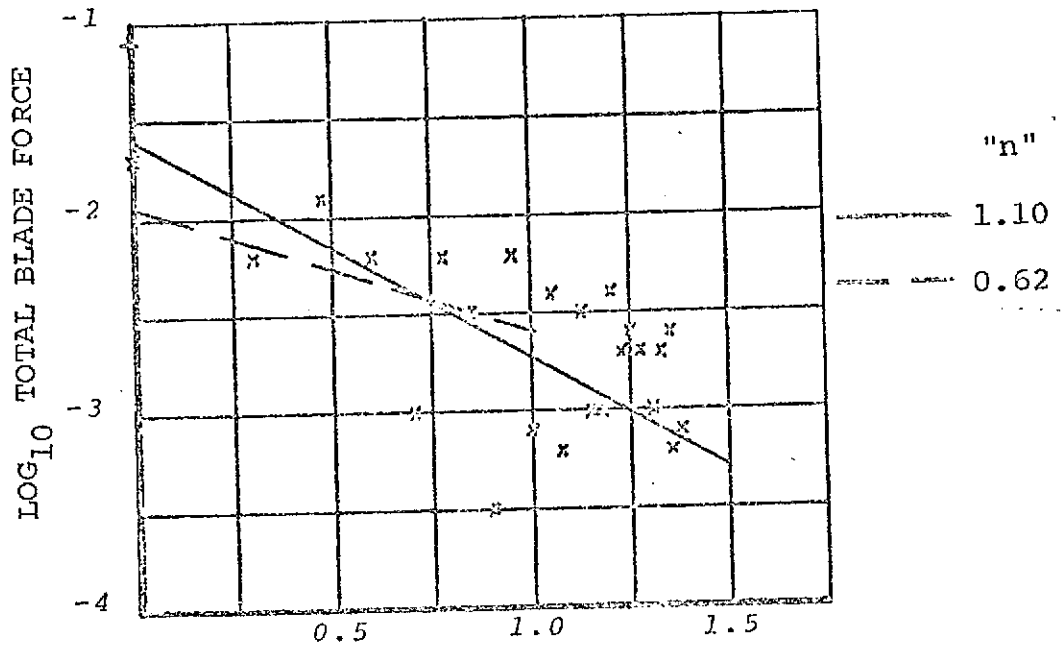
Figure 13. Correlation Results for Forward Flight
Run 18 Data Point 8 (Rotor Stalled)

f_{ff}
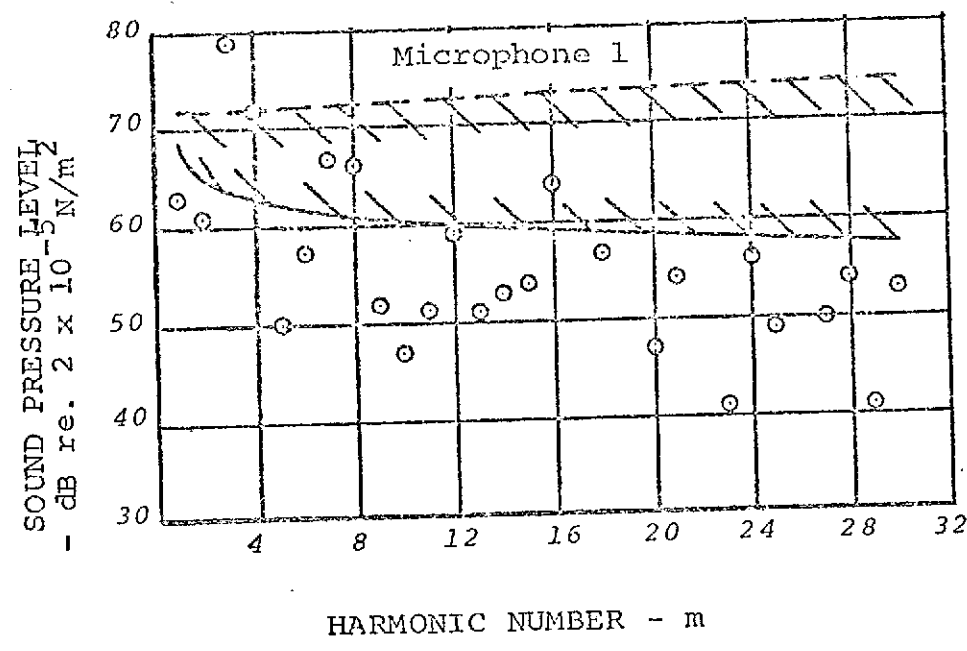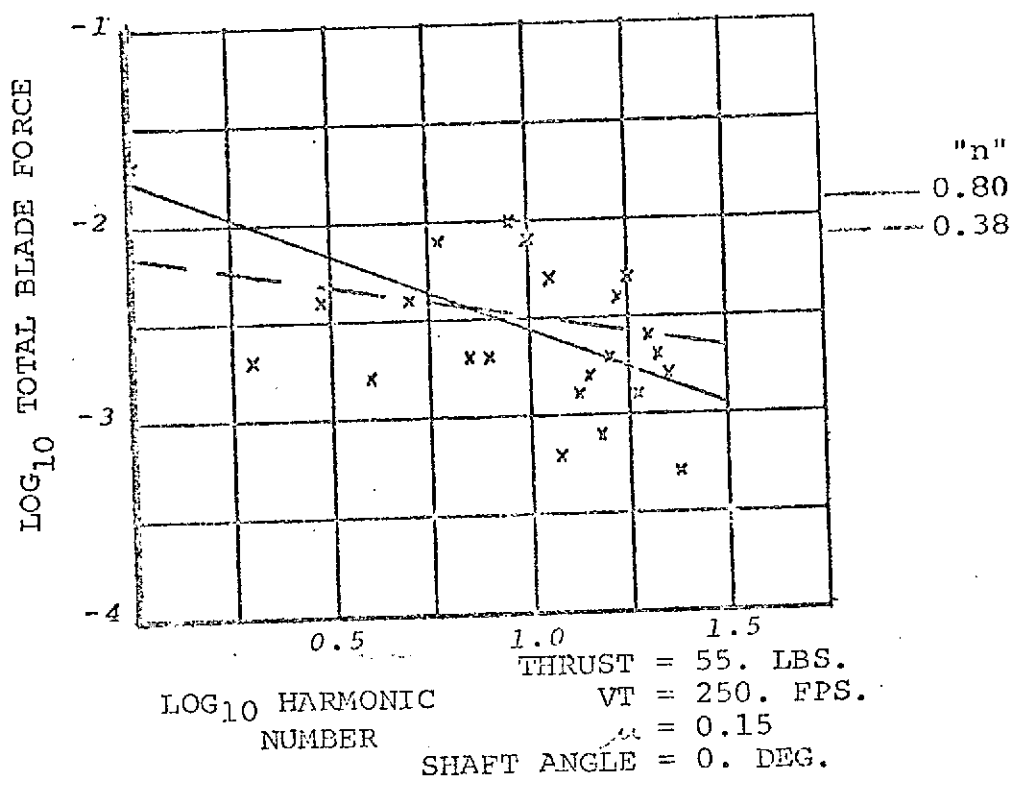
Figure 14. Correlation Results for Forward Flight
Run 18 Data Point 9 (Rotor Stalled)

The rotor shaft angle in this case is zero degrees.
Correlation with theory is fairly good and both pre-
dicted and measured data exhibit roughly the same
amount of scatter. The measured acoustic data falls
below the predicted levels for almost all harmonics.
It should be noted that the use of the lower pressure
slope results in a slightly increasing harmonic sound
pressure level as a function of sound harmonic number.
While this trend has been observed occasionally on
experimental rotor noise data, an indefinite increase
is unlikely and a drop-off in level occurs usually at
the medium to high noise harmonic numbers. Figure 15
shows that correlation with theory is very good for
Run 28 Data Point 10. The pressure data exhibits some-
what lower scatter than for data points 8 and 9.
Good correlation in general is exhibited by the data at
an advance ratio of 0.15 and a tip speed of 250 feet
per second. As with the hover data, it appears as if a
decay constant based on the steady pressure value would
have yielded an improved correlation.

Advance Ratio = 0.35; Tip Speed = 500 ft/sec: The
results for this test condition are given in Figures
16 through 23 for Run 28, Data Points 6 through
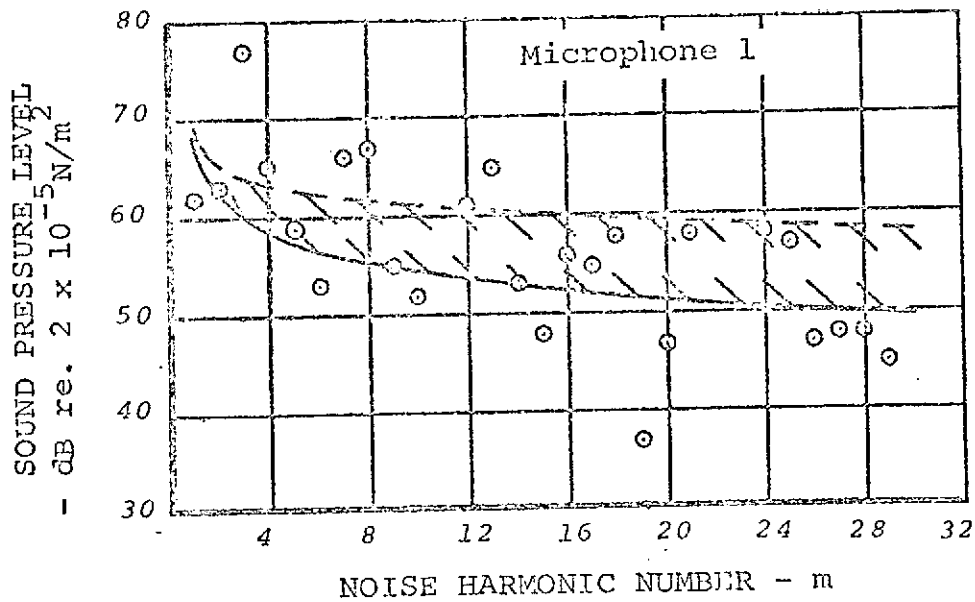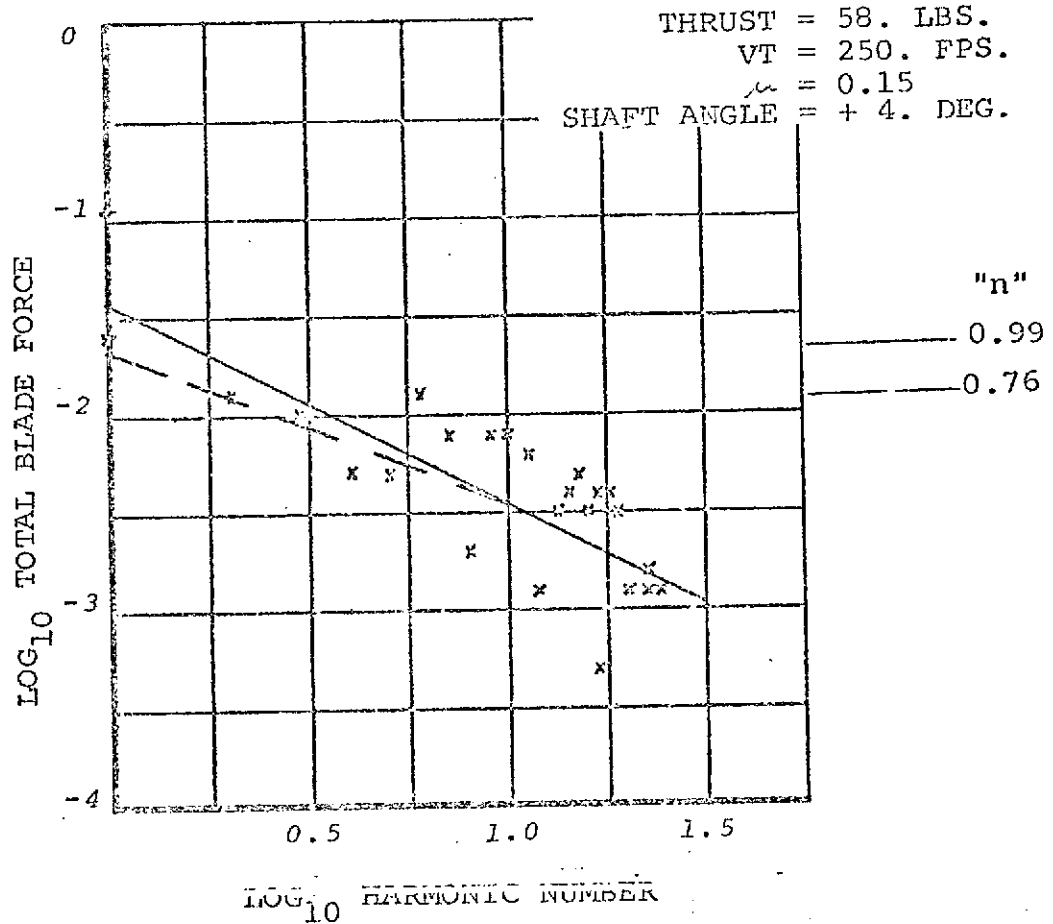13. Rotor shaft angle was varied from (-16) to (-1)

Figure 15.   Correlation Results for Forward Flight
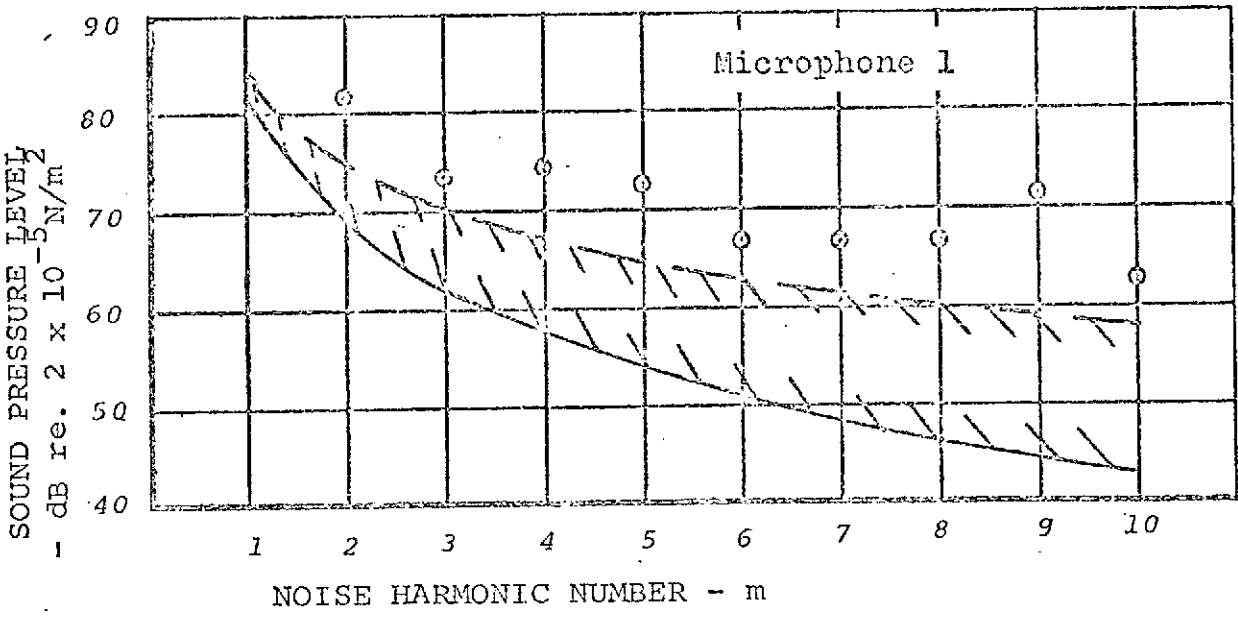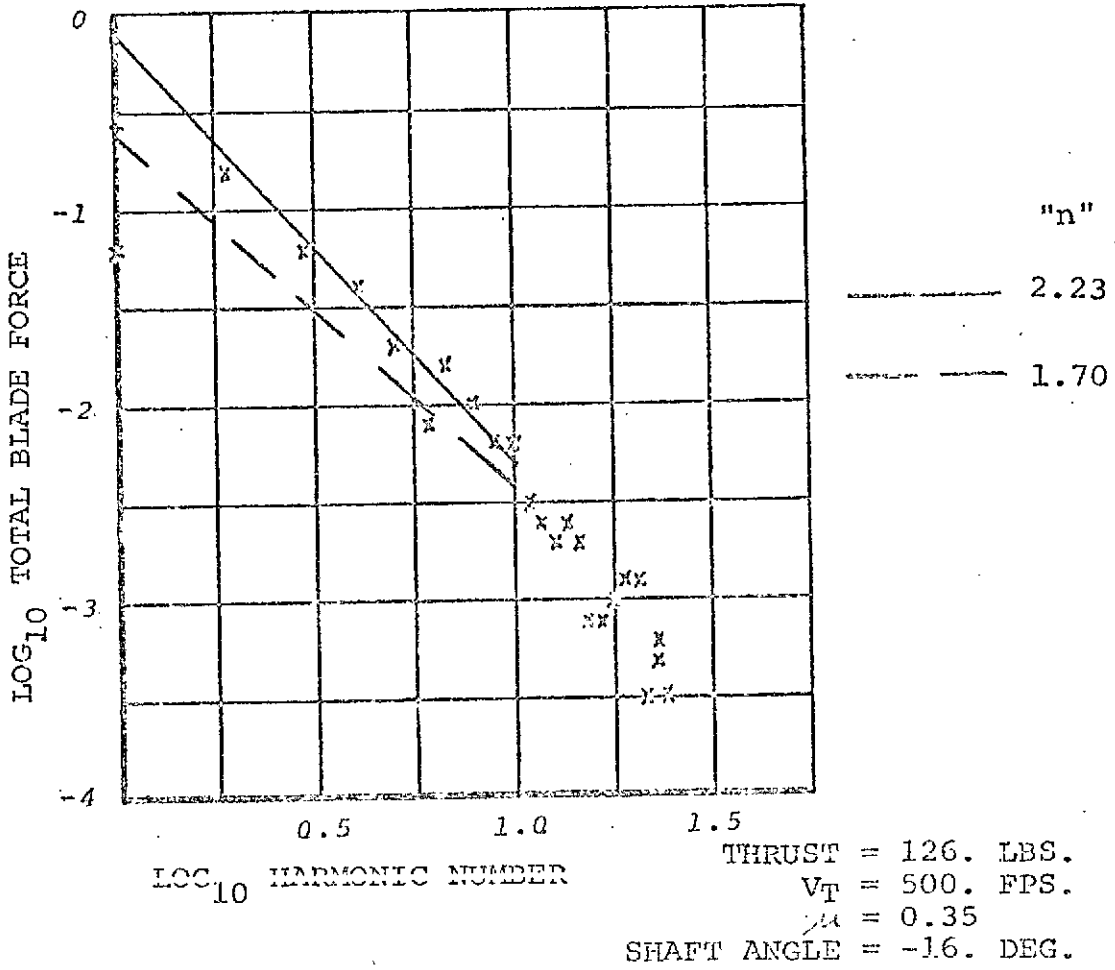Run 18 Data Point 10 (Rotor Stalled)

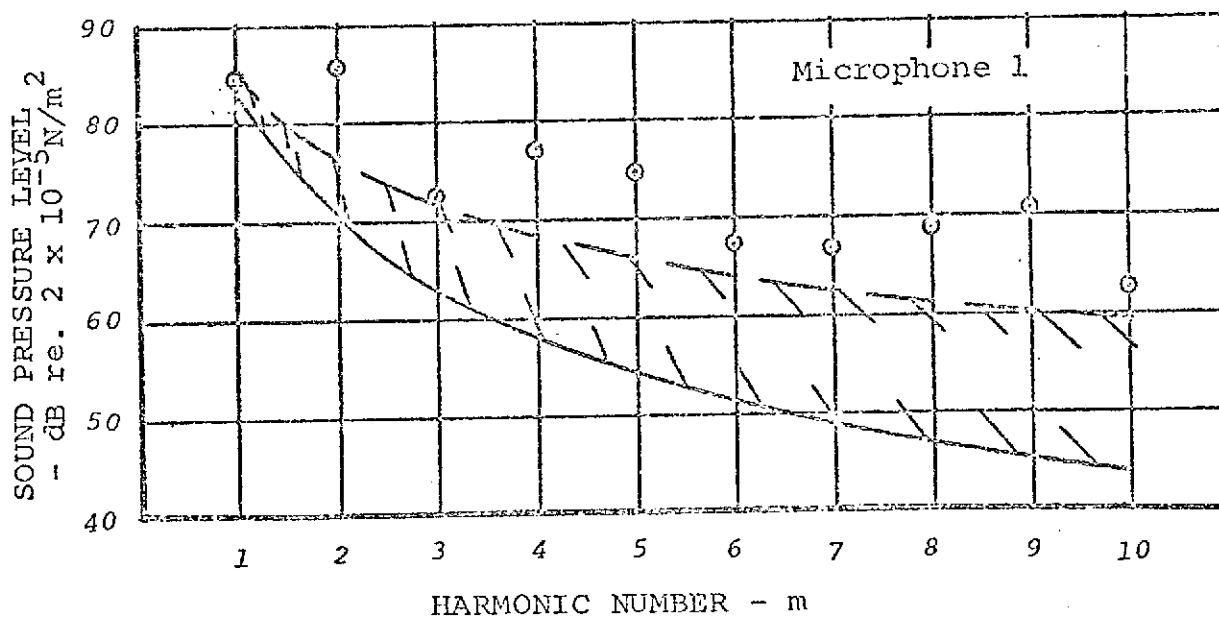Figure 16. Correlation Results for Forward Flight
Run 28 Data Point 6

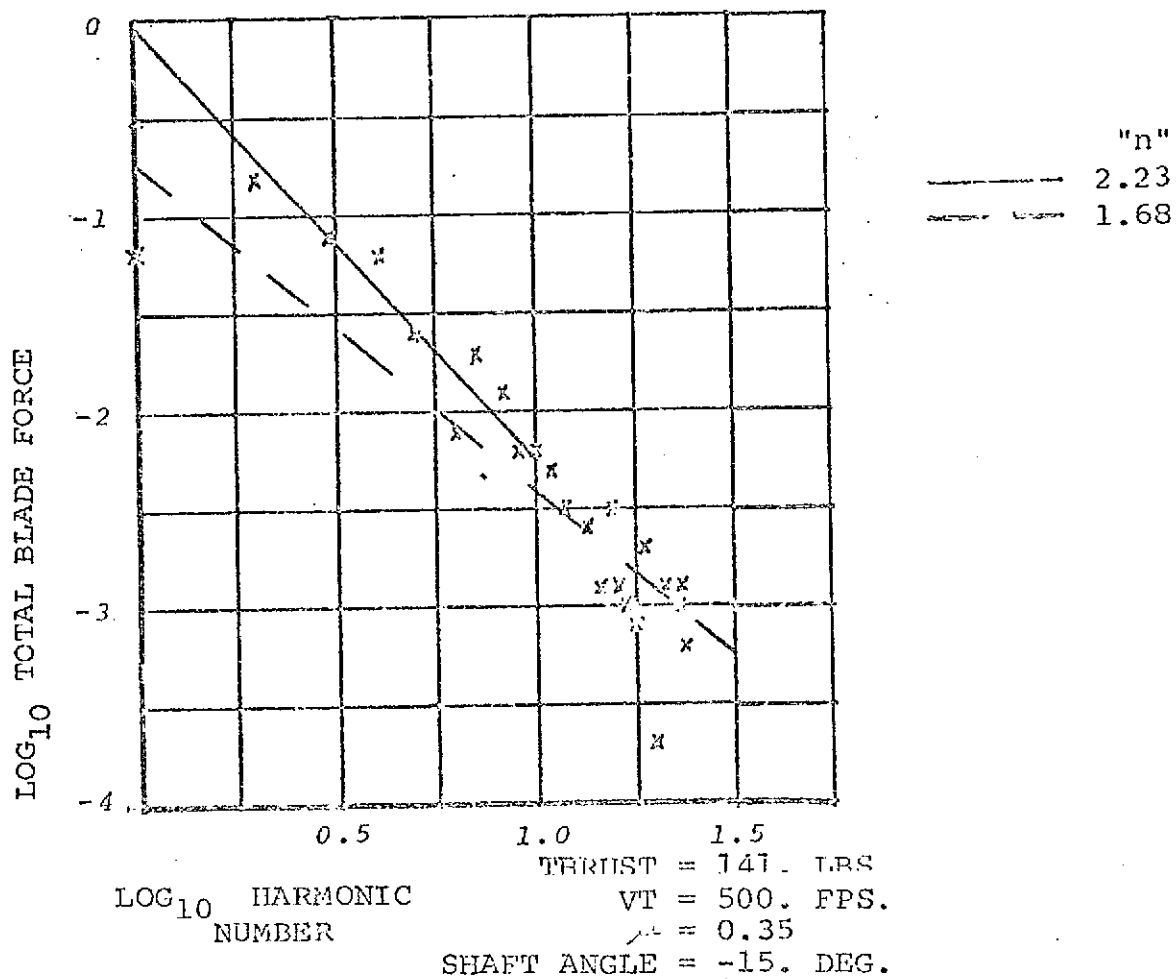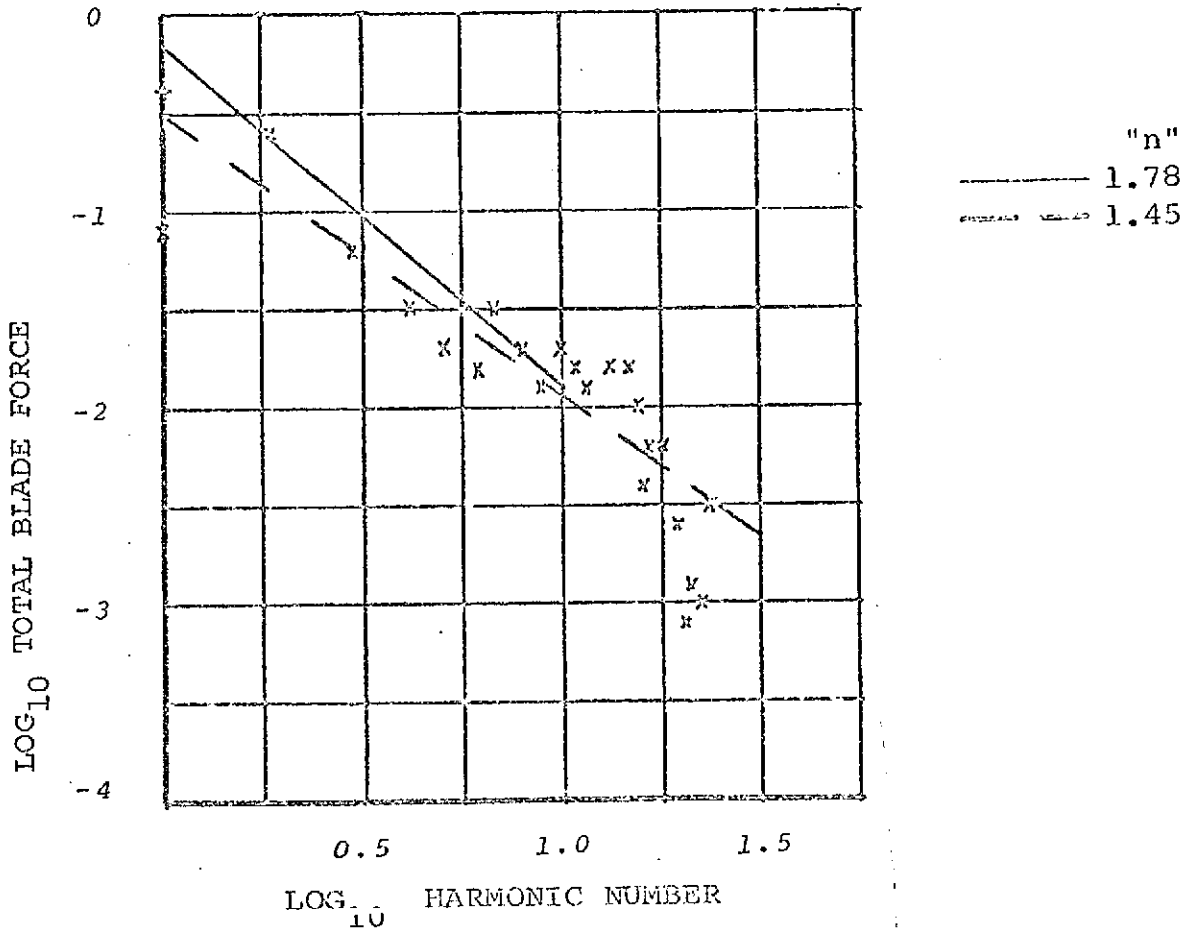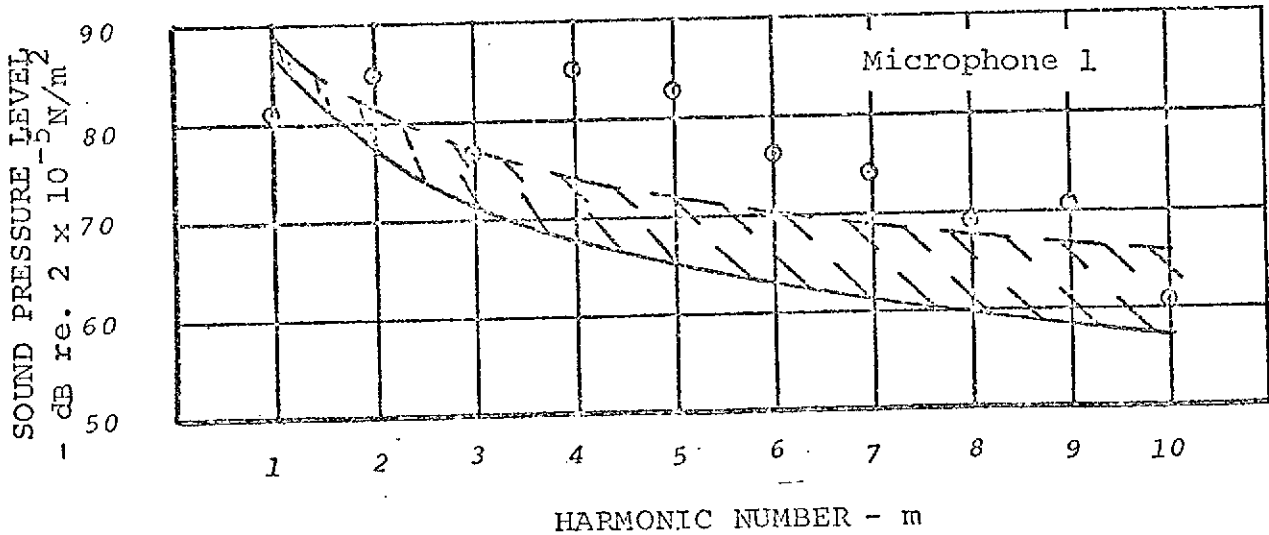Figure 17.   Correlation Results for Forward Flight
Run 28 Data Point 7

Figure 18. Correlation Results for Forward Flight
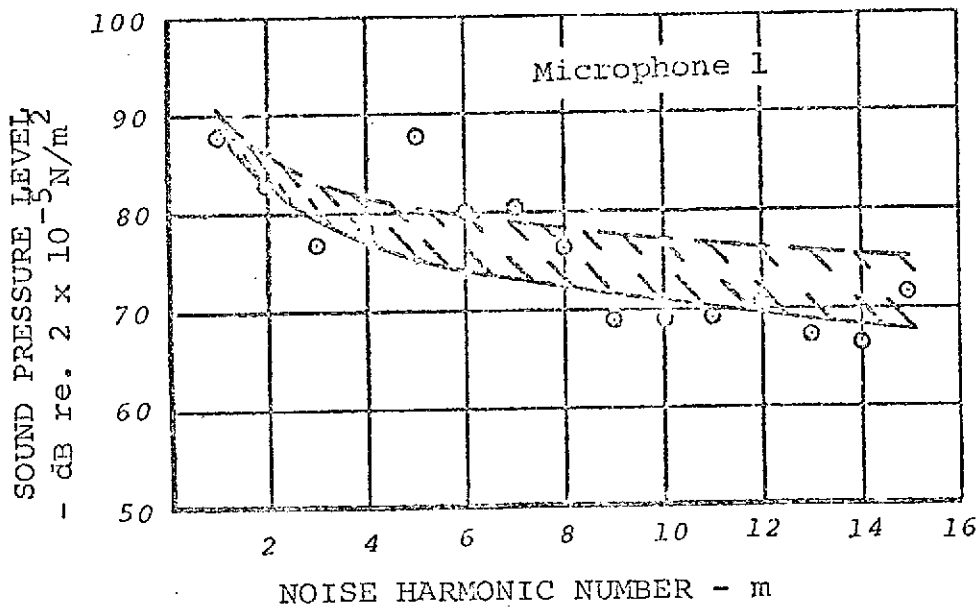Run 28 Data Point 8 (Rotor Stalled)

Figure 19. Correlation Results for Forward Flight
Run 28 Data Point 9. (Rotor Stalled)

Figure 20.   Correlation Results for Forward Flight Run
              28 Data Point 10   (Rotor Stalled)
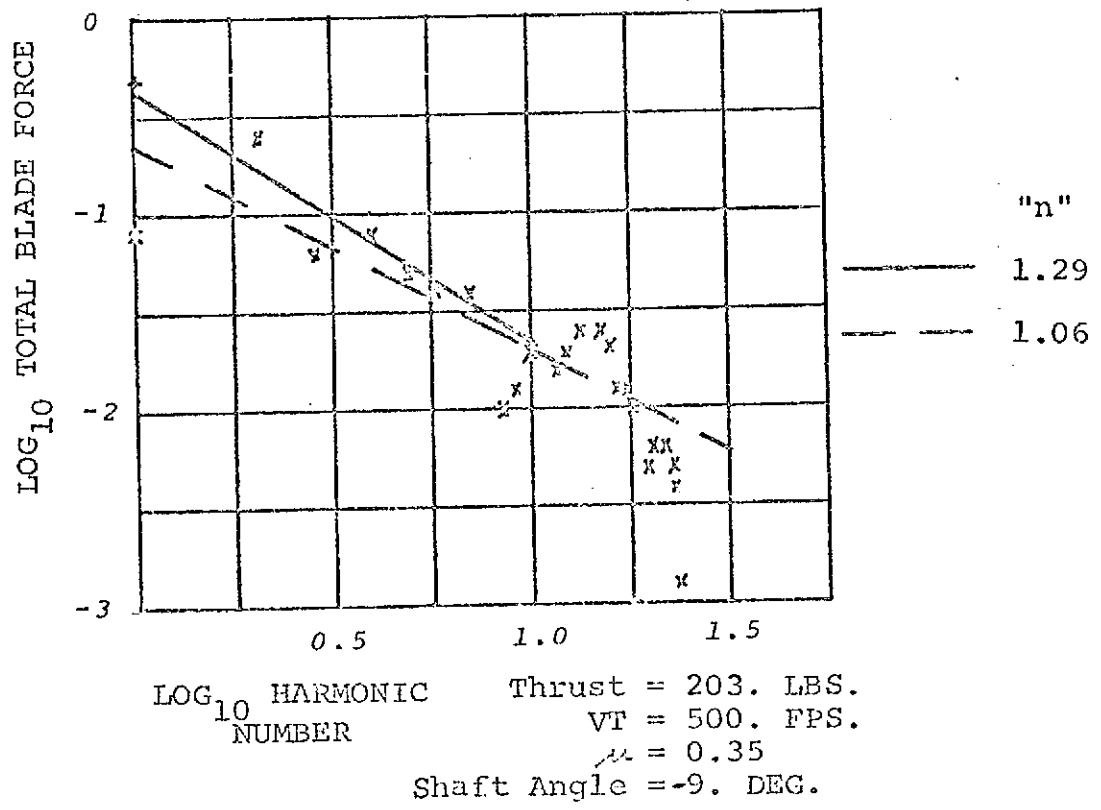
Figure 21. Correlation Results for Forward Flight
Run 28 Data Point 11 (Rotor Stalled)
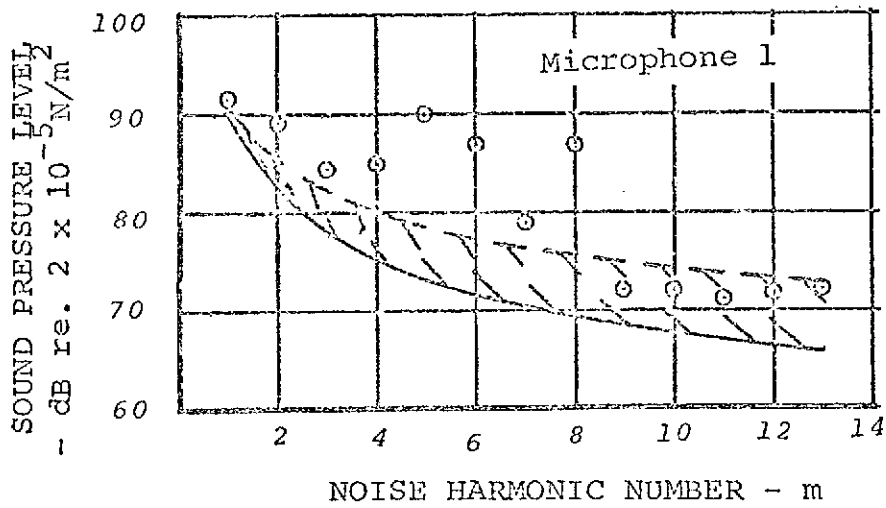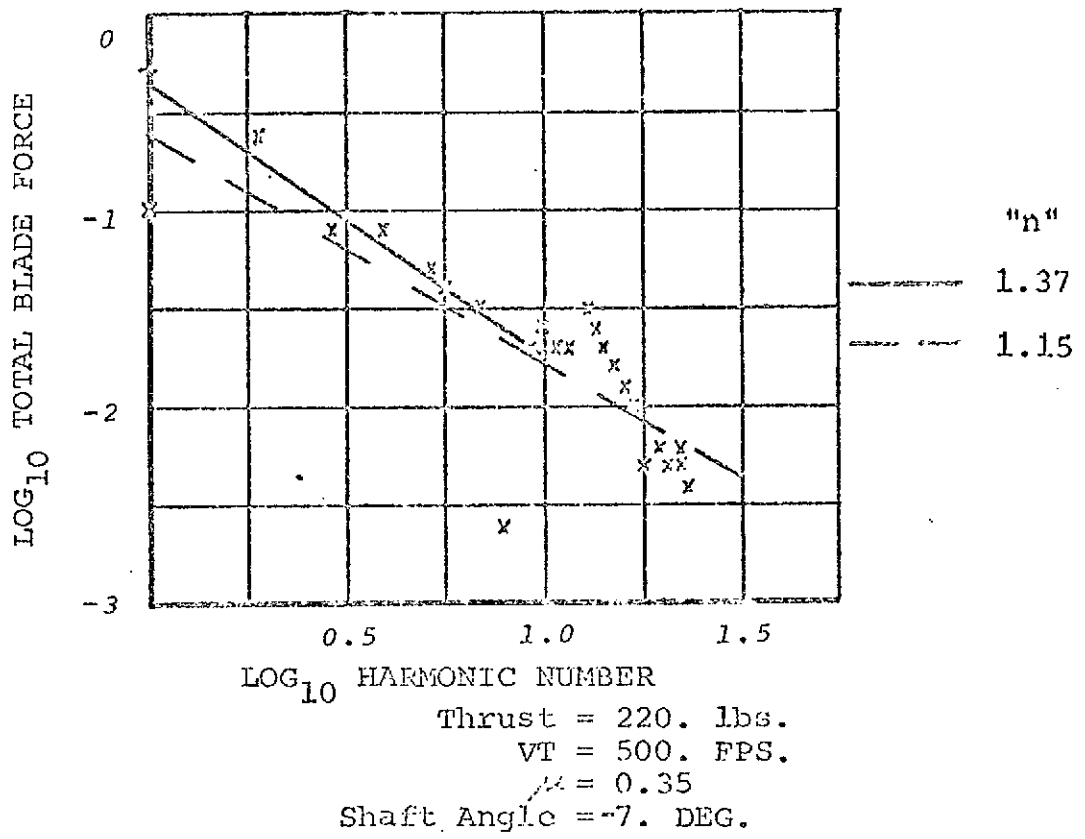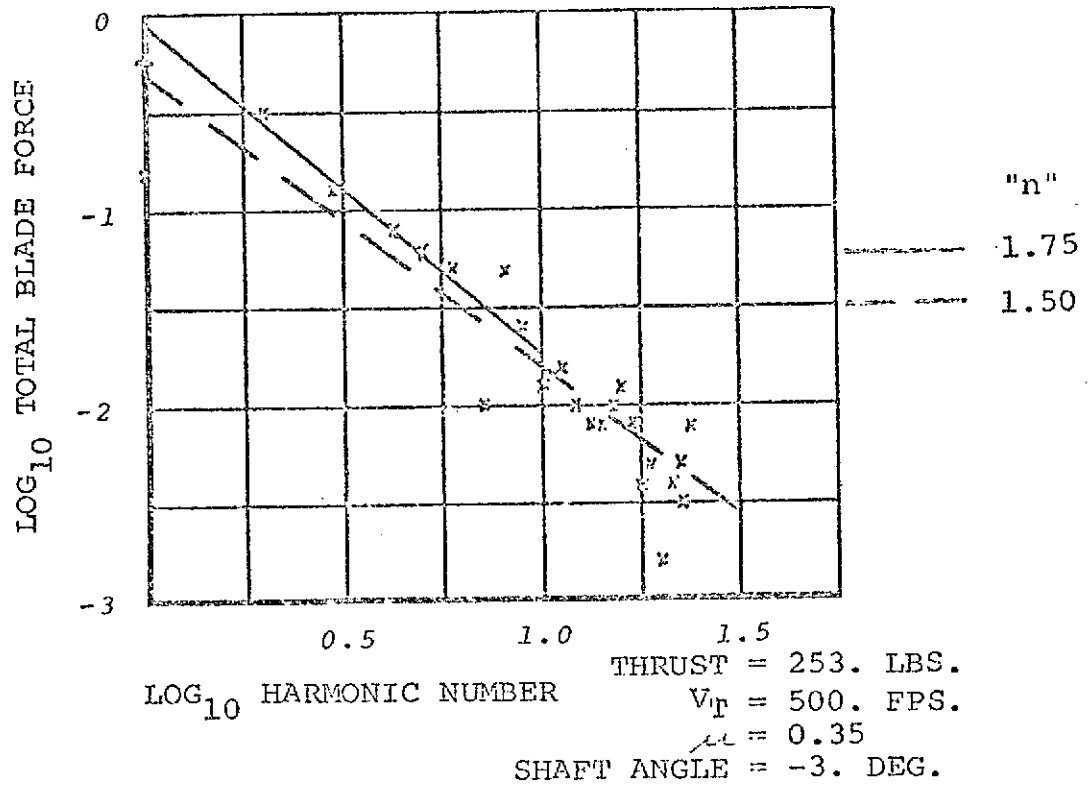
Figure 22. Correlation Results for Forward Flight
Run 28 Data Point 12   (Rotor Stalled)
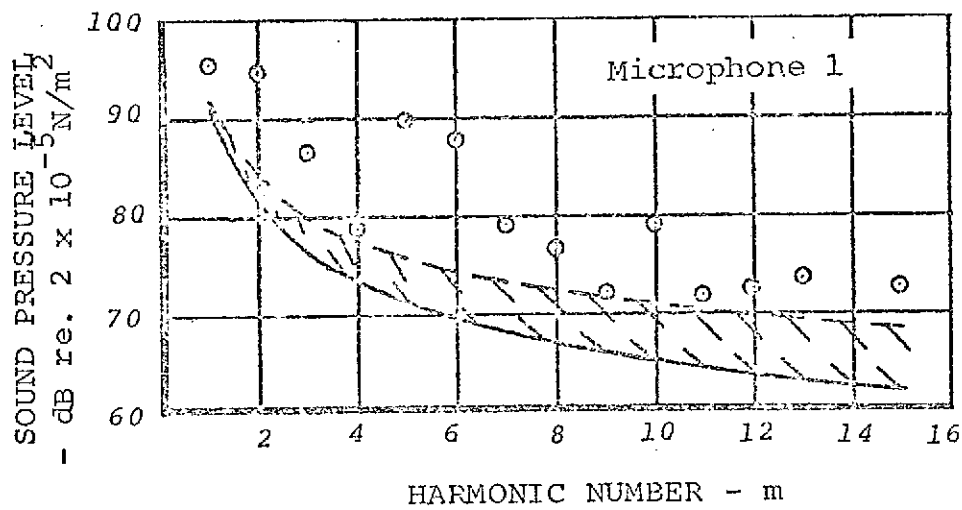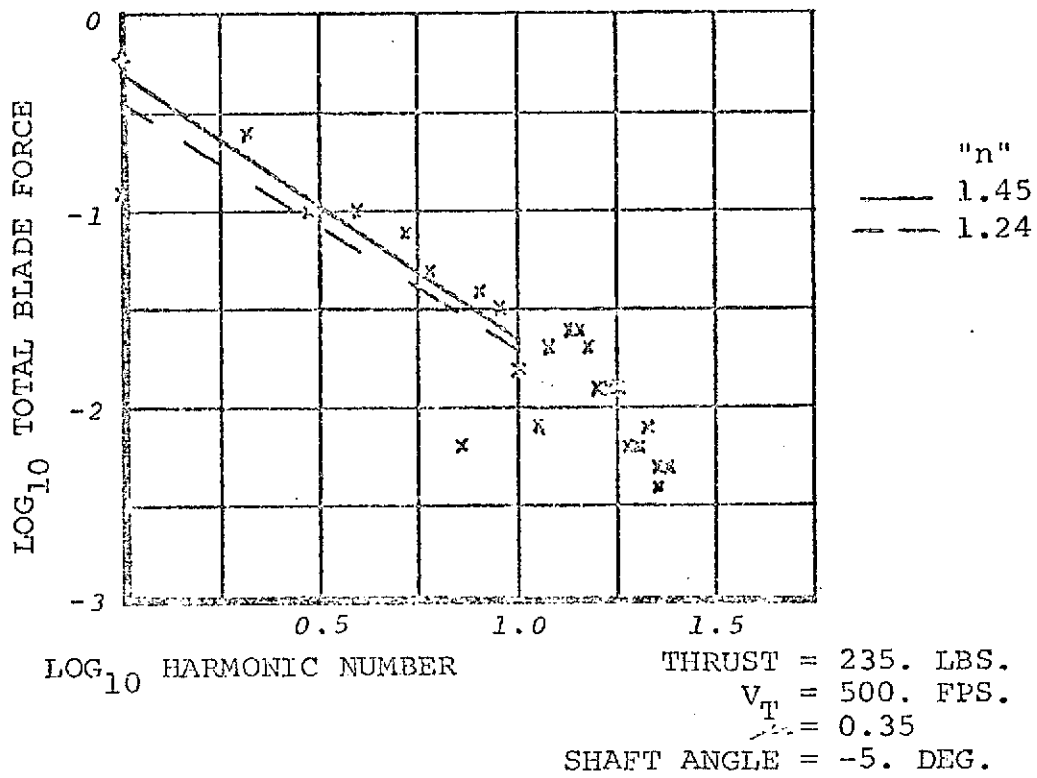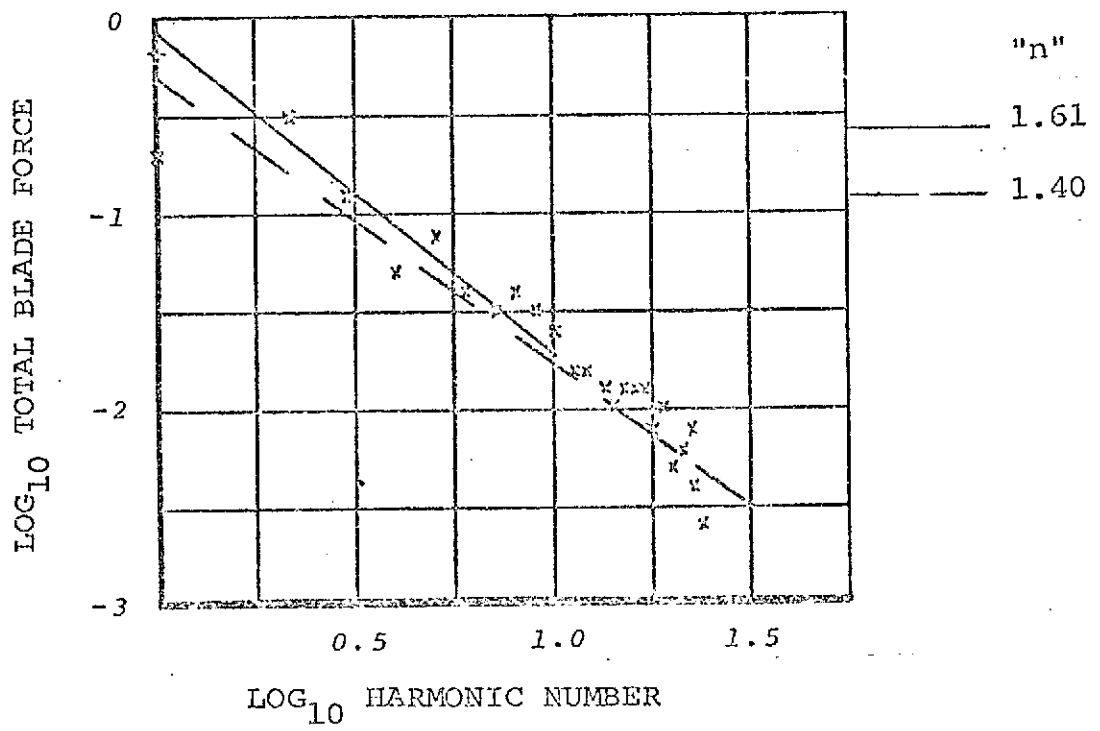
Figure 23.   Correlation Results for Forward Flight
Run 28 Data Point 13 (Rotor Stalled)
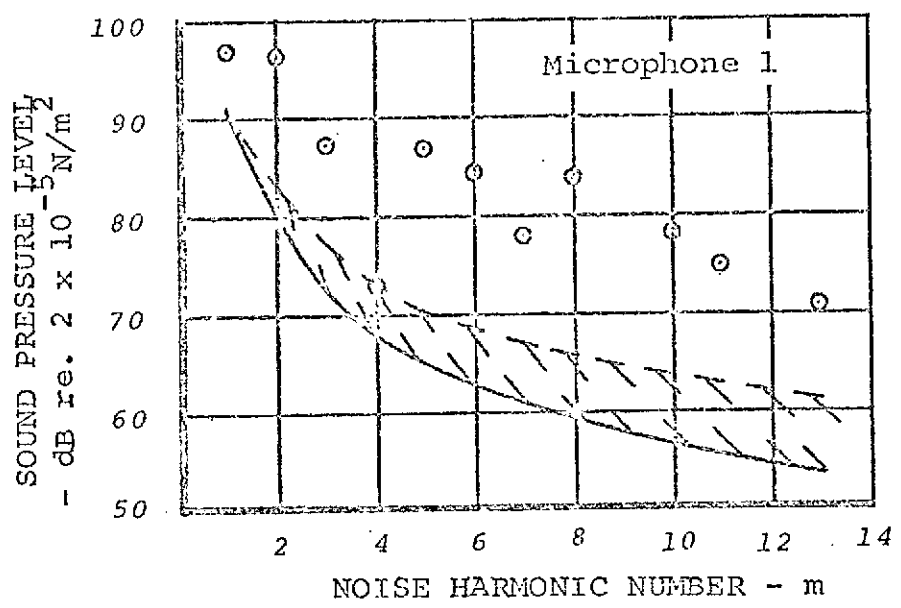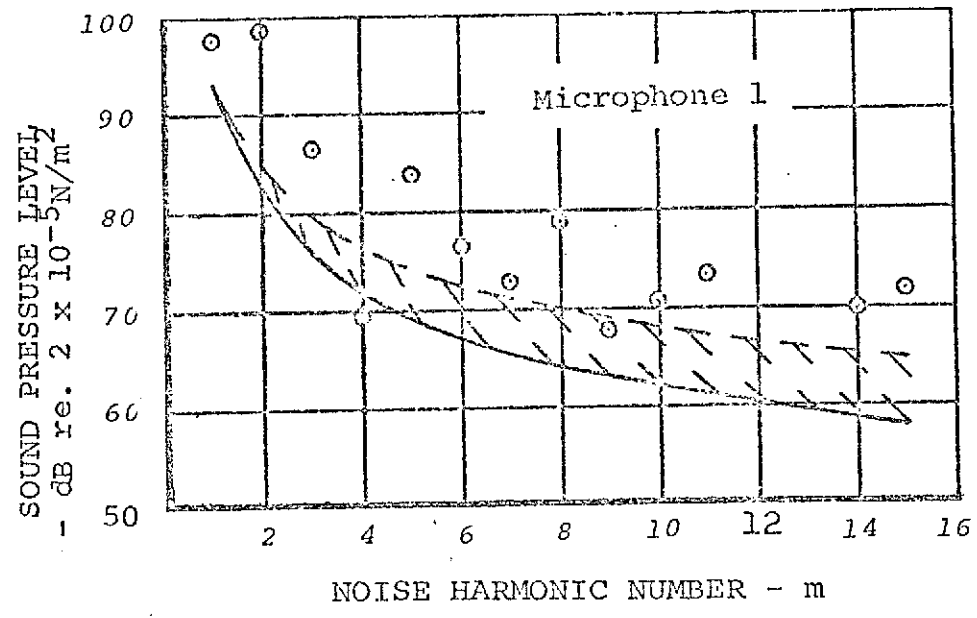
degrees, while thrust changed from 126 to 292
pounds.

Data Point 12 exhibits the greatest deviation of the
measured from the predicted noise data. Correlation
is good for data points 6, 7, 8, 11 and 13, the
measured acoustic data being within a 10 dB range of
the predicted scatter. Data Points 9 and 10 exhibit
excellent correlation with theory.

Overall correlation of acoustic data with theory for
this flight condition is very good. There is remark-
ably little scatter in the blade pressure data; but
even so, the higher rotational noise harmonic levels
are very sensitive to slight changes in pressure decay
slope, and exhibit a 10 to 15 dB predicted scatter.

It is interesting to observe in Figures 16 thru 23
that after the on-set of stall (Figure 18), approximately
the tenth through twentieth rotor load harmonics
increase in level relative to the fifth through ninth
harmonic. There is then a sharp drop-off in level near
the twentieth harmonic. This plateau effect in harmonic
level distribution is less pronounced at small rotor
shaft angles (Figures 22 and 23). Minima in harmonic load
load distribution appear to occur near the eighth and
twentieth harmonic. The structure off this harmonic

level distribution suggests a lobed amplitude envelope,

indicative of a pulsed rotor blade loading.   This in

turn leads to the conclusion that many of the higher

harmonics of blade loading probably have a fixed phase

relationship with respect to each other,   which not _yes!_

only influences the level of the resulting noise

radiation,   but also the noise directivity.

V. CONCLUSIONS

As a result of the rotor measurement program under-taken to correlate blade surface pressures to rotation-al noise, several conclusions are drawn which reflect on the theoretical noise formulation of a rotor in non-axial flight:

1. In general, good correlation of measured acoustical data with a modified rotational noise theory has been achieved using measured rotor blade pressure harmonic decay using a model rotor in a reverberant enclosure. Correlation was excellent at low thrust in hover, and in forward flight at an advance ratio of 0.35.

2. For most of the hover and low forward speed (advance ratio = 0.15) test data, correlation with the modified theoretical noise formulation could be improved on by ignoring the measured first harmonic of rotor blade pressure, and assigning to it the value of the measured

steady pressure. The value of this is not so much in improving the predicted level of the noise harmonics due to the first harmonic of blade pressure, but in deriving a pressure decay slope which, when forced through this new value of the first pressure harmonic, yields better correlation of high harmonic rotational noise theory with measured data. An examination of the higher forward speed (advance ratio = 0.35) blade pressure data reveals that the good correlation already achieved would not be adversely affected by this new assumption.

3. The lack of good correlation with rotational noise directivity implies that the theoretical model needs improving by considering the span-wise and azimuthal phasing of at least the lower harmonics of the blade loads more vigorously. The present theory assumes that spanwise phasing of these loads is random.

4. Correlation of measured noise data with theory is not necessarily better when the rotor is unstalled than when it is stalled. The

theory appears to adequately account for the

acoustic noise produced by the increased drag.

5. *Increased confidence in the degree of correlation*

    between theory and data is provided by "banding"

    the scatter of the blade pressure and acoustic

    data. The cause of scatter in both pressure and

    acoustic data, however, needs to be more carefully

    identified and investigated for a further increase

    in correlation with theory.

Boeing Vertol Company

Philadelphia, Pa.

September 15, 1973

REFERENCES

1. Lowson, M.V.; and Ollerhead, J.B.: Studies of Helicopter Rotor Noise. USA AVLABS, TR 68-60, Jan., 1969.

2. Schmitz, F.H.; Stepniewski, W. Z.; Gibs, J.; and Hinterkeuser, E.: A Comparison of Optimal and Noise-Abatement Trajectories of a Tilt-Rotor Aircraft. U.S. Army Air Mobility R&D Laboratory, Ames Directorate and Ames Research Center, Report NASA CR-2034, May, 1972.

3. Gutin, L.: On the Sound Field of a Rotating Propeller. Langley Aeronautical Laboratory, NASA TM-1195, Oct. 1948.

4. Garrick, I.E.; and Watkins, C.E.: A Theoretical Study of the Effect of Forward Speed on the Free-Space Sound-Pressure Field around Propellers. NACA Report 1198, 1954.

5. Ollerhead, J.B.; and Lowson, M.V.: Problems of Helicopter Noise Estimation and Reduction. AIAA Paper No. 69-195, Feb. 1969.

6. Scheiman, J.: A Tabulation of Helicopter Rotor-Blade Differential Pressures, Stresses and Motions as Measured in Flight, Langley Research Center Report TMX-952, Mar. 1954.

7. Burpo, F. B.; and Lynn, R.R.: Measurement of Dynamic Airloads on a Full-Scale, Semi-Rigid Rotor. Bell Helicopter Co., AVLABS Report TCREC TR-62-42, Dec. 1962.

8. Fisher, R.K.; Tompkins, J.E.; Bobo; C.J.; and Child, R.F.: An Experimental Investigation of the Helicopter Rotor Blade Element Airloads on a Model Rotor in the Blade Stall Regime. Boeing Vertol Company Report D210-10347-1; Sept. 1971.

9. Hinterkeuser, E.: Correlation of Wind Tunnel and Free-Field Acoustical Data. Boeing Vertol Company Report IOM 8-7446-4-810, Sept. 1970.

Acoustical Properties of a Model Rotor

in Non-Axial Flight

By

E. Hinterkeuser

Boeing Vertol Company

SUMMARY

A wind tunnel measurement program was performed on
a model rotor to measure blade loads and the acoustical
noise emitted by the model. The purpose of the
efforts described in this report was to correlate a
theoretical formulation of the rotational noise of a
rotor in non-axial flight with the measured loads and
noise of the rotor in the test program. The results
indicate to what extent the theoretical noise formu-
lation has been successful in predicting the acoustic
behavior of the model rotor.

Test results indicate that, in general, good correla-
tion between theory and data was achieved using actual
measured rotor blade pressure harmonic decay levels
and lift, drag and radial force magnitudes.

Both pressure and acoustic data exhibited considerable
scatter in hover and low speed forward flight which

resulted in a fairly wide latitude in the noise level
prediction at higher harmonics. In most cases, the
level of the first harmonic of blade loading appeared
low and should probably be ignored in deriving a
loading harmonic decay rate for use in the theoretical
noise model. The substitution of the magnitude of the
rotor steady pressure for the level of the first
harmonic seems warranted in view of the increase in
correlation afforded. It also appears that a con-
sideration of blade load span-wise and azimuthal phasing
would both contribute to a better understanding of rotor
noise directivity effects.